THE NATIONAL ACADEMIES PRESS

This PDF is available at http://nap.edu/14556

SHARE

Summary of Cast-In-Place Concrete Connections for Precast Deck Systems

BUY THIS BOOK

FIND RELATED TITLES

DETAILS

32 pages | | PAPERBACK

ISBN 978-0-309-21328-8 | DOI 10.17226/14556

AUTHORS

Visit the National Academies Press at NAP.edu and login or register to get:

– Access to free PDF downloads of thousands of scientific reports

– 10% off the price of print titles

– Email or social media notifications of new titles related to your interests

– Special offers and discounts

Distribution, posting, or copying of this PDF is strictly prohibited without written permission of the National Academies Press. (Request Permission) Unless otherwise indicated, all materials in this PDF are copyrighted by the National Academy of Sciences.

Copyright © National Academy of Sciences. All rights reserved.

July 2011

NATIONAL COOPERATIVE HIGHWAY RESEARCH PROGRAM

Responsible Senior Program Officer: Waseem Dekelbab

Research Results Digest 355

SUMMARY OF CAST-IN-PLACE CONCRETE CONNECTIONS FOR PRECAST DECK SYSTEMS

This digest summarizes key findings from NCHRP Project 10-71 "Cast-in-Place Concrete Connections for Precast Deck Systems," conducted by the University of Minnesota–Twin Cities and the University of Tennessee–Knoxville. The digest was prepared from the project final report (published as *NCHRP Web-Only Document 173: Cast-in-Place Concrete Connections for Precast Deck Systems)* authored by Catherine French, Carol Shield, Z. John Ma, David Klaseus, Matthew Smith, Whitney Eriksson, Peng Zhu, Samuel Lewis, and Cheryl E. Chapman.

CONTENTS

Introduction, 1

PCSSS, 2

Longitudinal and Transverse Joints in DBT and Full-Depth Precast Panel on Girder Systems, 16

References for PCSSS Portion of Study, 31

References for Longitudinal and Transverse Joints In DBT And Full-Depth Precast Panel on Girder System Portion of Study, 31

INTRODUCTION

The aging highway bridge infrastructure in the United States is subjected to increasing traffic volumes and must be continuously renewed while simultaneously accommodating traffic flow. Speed of construction, especially for the case of bridge replacement and repair projects, is a critical issue. Disruption of traffic and inconvenience to motorists, not to mention major safety issues arising from detours, has encouraged the development of rapid construction methods. The issue of construction speed, combined with higher labor costs and more variable quality control associated with on-site concrete casting, construction and motorist safety issues, political pressures, and environmental concerns, has paved the way for further increase in the use of precast elements.

Depending on the specific site conditions, the use of prefabricated bridge systems can minimize traffic disruption, improve work-zone safety, minimize impact to the environment, improve constructability, increase quality, and lower life-cycle costs. This technology is applicable and needed for both existing bridge replacement and new bridge construction. For many deficient bridges in the United States on the waiting list for replacement, it is imperative that new bridge construction be as economical as possible and yet be long lasting and nearly maintenance free.

The focus of the research was to develop recommended design and construction specifications and examples for the design and construction of durable cast-in-place (CIP) reinforced concrete connections for precast deck systems. These connections were to emulate monolithic construction and consider issues including durability and fatigue, while increasing speed of construction. The typical sequence of erecting bridge superstructures in the United States is to erect the precast prestressed concrete or steel beams, place either temporary formwork or stay-in-place formwork such as steel or concrete panels, place deck reinforcement, cast deck concrete, and remove formwork if necessary. This project focused on systems that reduce the need to place and remove formwork, thus accelerating on-site construction and improving safety.

The three systems considered to accomplish these objectives were identified during a 2004 Prefabricated Bridge Elements and

TRANSPORTATION RESEARCH BOARD
OF THE NATIONAL ACADEMIES

Copyright National Academy of Sciences. All rights reserved.

Systems International Scanning tour. These systems included (1) a precast composite slab span system (PCSSS) for short to moderate span structures based on the French Poutre Dalle system, (2) full-depth prefabricated concrete decks, and (3) deck joint closure details [e.g., decked-bulb-T (DBT) flange connections] for precast prestressed concrete girder systems for long span structures. Each system uses precast elements that are brought to the construction site ready to be set in place and quickly joined together. Depending on the system, the connections are either transverse (i.e., across the width of the bridge) or longitudinal (i.e., along the length of the bridge). The first system, PCSSS, is an entire bridge system whereas the other two systems investigated in the project represent transverse and longitudinal joint details that transfer moment and shear in precast deck panels and flanges of DBTs. Because of the similarities in the latter two types of systems, they are grouped together in this summary. Two types of connection concepts were explored with these details: looped bar details and two layers of headed bar details. Although both types of systems performed adequately in initial tests, the looped bar systems were deemed to be more practical for construction purposes and were investigated in the subsequent tests.

Because this report covers two very different systems: (1) the PCSSS, which is an entire bridge system, and (2) transverse and longitudinal CIP connection concepts that transfer moment and shear between precast deck panels and the flanges of precast DBTs, this summary, as well as the report, is separated accordingly. The complete report including appendices is available on the TRB website as *NCHRP Web-Only Document 173* (http://www.trb.org/Main/Blurbs/164971.aspx).

PCSSS

Introduction

PCSSSs are a promising technology for the implementation of accelerated construction techniques for bridge construction. These bridge systems are composed of precast, inverted-T sections, fabricated off-site and delivered to the jobsite ready for erection. The inverted-T sections are assembled such that no formwork is required prior to the placement of the CIP deck, which considerably reduces construction time related to the placement and removal of formwork. Figure 1 shows the construction of one of the initial implementations of the PCSSS in Center City, Minnesota. Transverse load transfer is achieved through the development of transversely oriented reinforcement protruding from the precast members. Furthermore, improved quality of the main superstructure can be achieved because of the rigid quality control associated with the fabrication of precast members, which may be difficult to achieve in CIP bridge construction.

Figure 2 shows a representative cross section of a precast inverted-T section used in the construction of the PCSSS. The precast sections are placed adjacent to each other such that the transverse hooked bars protruding from the adjacent webs form a lap splice in the CIP region between the webs.

One of the issues investigated in the NCHRP Project 10-71 study was the durability of the PCSSS, specifically its ability to control potential reflective cracks that might develop in the CIP concrete due to the discontinuity created at the interface between the adjacent flanges that abut or due to the corners of the precast web. A supplemental reinforcement cage is dropped into the CIP region between webs to provide supplemental reflective crack control above the interface between the adjacent flanges. Figure 3 shows a cross section of the PCSSS indicating the potential locations where reflective cracking would be expected to initiate. Figure 4 shows a typical instrumentation plan used in the investigation to monitor initiation of any reflective cracks that might have developed.

Research Methodology and Findings

Several numerical and experimental investigations were completed and reviewed during the project that related to issues of importance to the design and performance of PCSSS bridges. Included in this review was the work completed during a study commissioned by Mn/DOT, which was the first DOT in the United States to implement this technology. The laboratory bridge specimen utilized during the Mn/DOT study was subsequently made available for use with the project described herein.

Numerical studies included an investigation of bursting and spalling stresses in the end zones of precast inverted-T sections, effects of spacing of transverse reinforcement in the joint region, and an investigation of the applicability of current design specifications for slab-type bridges to the design of PCSSS bridges for live load distribution factors and

Copyright National Academy of Sciences. All rights reserved.

Figure 1 Sequence of construction of a PCSSS: (a) precast pier caps in place, (b) Inverted T-sections in place (elevation view), (c) Inverted T-sections in place (plan view), (d) drop-in cage placed between precast webs for potential crack control, (e) deck reinforcement in place, and (f) finished structure.

for consideration of effects of skewed supports. The two primary considerations that distinguish PCSSS bridges from slab-span bridges are (1) the required reinforcement to control reflective cracking above the longitudinal joint between the precast flanges and (2) the effect of time-dependent restraint moments due to the composite nature of the system. With regard to the issue of reflective crack control, in addition to a numerical investigation as to the effect of the transverse reinforcement, the issue was also studied in laboratory investigations of two large-scale laboratory specimens (i.e., Concept 1 and 2 bridges), as well as in subassemblage test specimens specifically designed to investigate crack control.

Copyright National Academy of Sciences. All rights reserved.

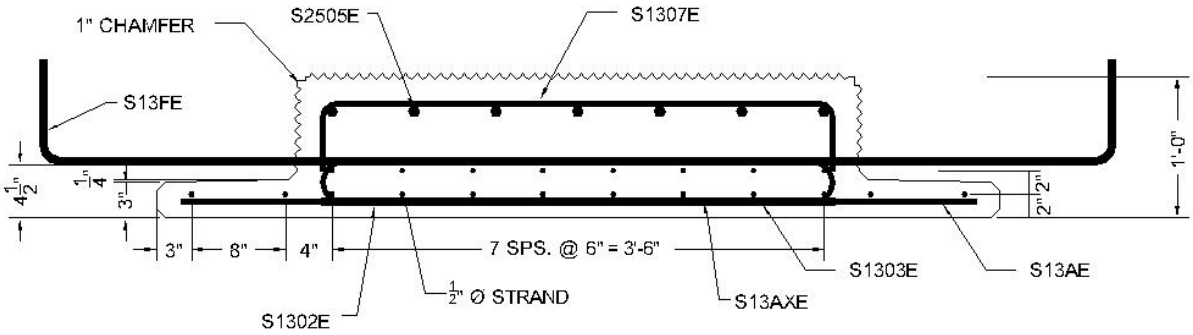

Figure 2 PCSSS precast inverted-T cross section.

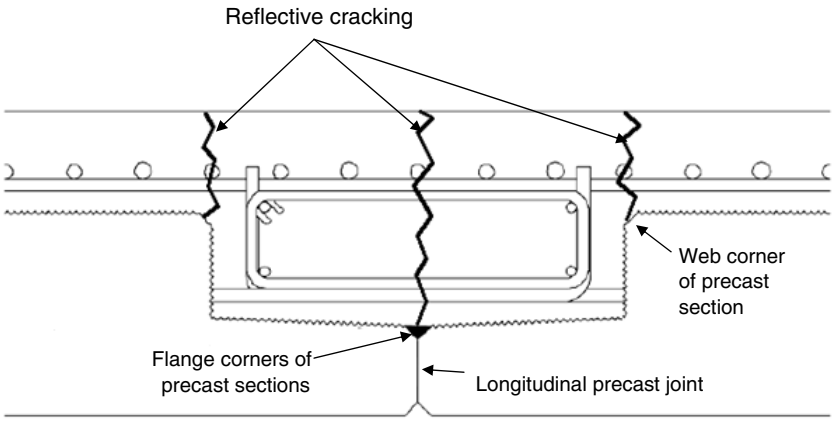

Figure 3 Anticipated locations of reflective cracking in Minnesota Department of Transportation (Mn/DOT) PCSSS (Bell et al. 2006).

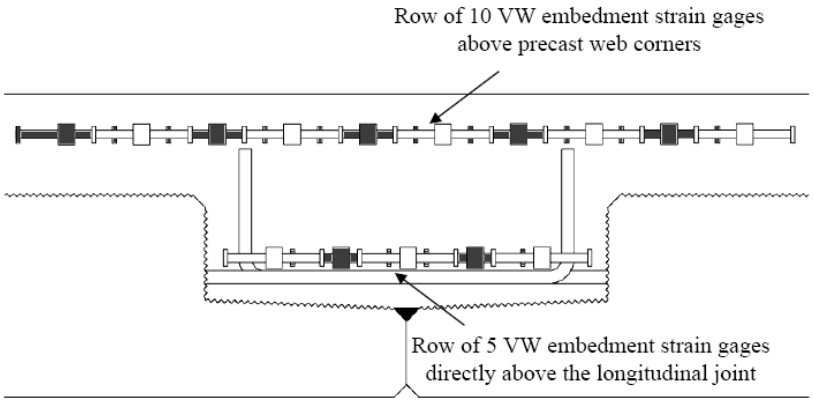

Figure 4 Location of transverse concrete embedment gages in each of the three instrumented joints at midspan of the center span of the Center City Bridge (Bell et al. 2006) (VW = vibrating wire).

Copyright National Academy of Sciences. All rights reserved.

The Concept 1 laboratory bridge was a two-span continuous bridge that included variations in a number of parameters, including precast flange depth and end zone reinforcement details. It had been instrumented in the study for the Mn/DOT to investigate the effects of restraint moment and potential development of reflective cracking. The Concept 1 specimen included No. 6 transverse hooked reinforcement embedded into the precast webs to provide load transfer and crack control in the joint region, as well as No. 5 cage stirrups that contributed to the crack control reinforcement. The nominal maximum spacing between transverse reinforcement was 12 in., similar to the detail of one of the first implementations of PCSSS bridges in the State of Minnesota, the Center City Bridge. The variations in the detailing of the two spans in the Concept 1 bridge are summarized in Table 1. The Concept 2 bridge was a simply supported structure that included variations in the transverse reinforcement details across the precast joint. The horizontal shear reinforcement between the precast web and CIP topping was eliminated in this structure. In the Concept 2 specimen, No. 4 embedded hooked reinforcement was used in the west half of the simple span, while No. 4 straight embedded bars mechanically connected to reinforcement in the precast webs were provided in the east half span. See Figure 2 for illustration of the precast inverted-T cross section used in the west end of the precast beams 1N and 1S in the Concept 2 laboratory bridge specimen. No. 3 cage stirrups were staggered in the Concept 2 laboratory bridge relative to the transverse reinforcement spaced at 18 in. to provide a maximum spacing of 9 in. between transverse reinforcement.

Figure 5 shows the instrumentation layout in the plan view of the Concept 1 bridge. A similar instrumentation configuration was used in the Concept 2 bridge.

The performance of both bridge specimens was investigated under various types of loading, including cyclic loading to simulate traffic, loading to simulate environmental effects, and loading to investigate load transfer between adjacent precast panels (both longitudinal and transverse). To simulate the environmental (thermal gradient) effects—as observed in the Center City Bridge that was instrumented for the Mn/DOT study—the structures were loaded to impose transverse strains above the longitudinal joint between the precast flanges. The structures were cycled at these strain levels to simulate more than 100 years of service life as exposed to thermal gradient effects, which were found to be much more significant than strains due to traffic loading. Following the cyclic load tests, the bridges were loaded above the nominal design flexural strengths to the limiting capacities of the actuators to investigate the effectiveness of composite action. Following the tests, cores and slices of the bridge were examined to investigate any residual cracks.

Figure 6 shows the location of the patch loads in the Concept 1 bridge used to investigate the effect of cyclic loading to simulate approximately 2 million cycles of vehicle loading over the joint. Relatively small strains were observed in those tests. As a

Table 1 Original and modified design criteria in Spans 1 and 2 of the Concept 1 laboratory bridge.

Span 1 (Modified Section)	Span 2 (Original Section)
Decreased flange thickness (3 in.)	Original flange thickness (5¼ in.)
Smooth flange surface	Original roughened flange surface
Increased stirrup spacing for horizontal shear reinforcement (No. 5 stirrups at 24 in.)	Original stirrup spacing for horizontal shear reinforcement (No. 5 stirrups at 12 in.)
Increased clear spacing under hooks (1⅜ in. nominal clear spacing between horizontal shear reinforcement stirrups and precast section)	Original clear spacing under hooks (¼ in. nominal clear spacing between horizontal shear reinforcement stirrups and precast section)
Decreased transverse deck reinforcement (No. 4 bars at 12 in.)	Original transverse deck reinforcement (No. 5 bars at 12 in.)
The longitudinal deck steel in the south half of the bridge was two No. 7 and one No. 8 bars per 12 in. at the continuous pier (Original design)	
The longitudinal deck steel in the north half of the bridge was reduced to No. 6 bars at 6 in. spacing at the continuous pier (Modified design)	

Copyright National Academy of Sciences. All rights reserved.

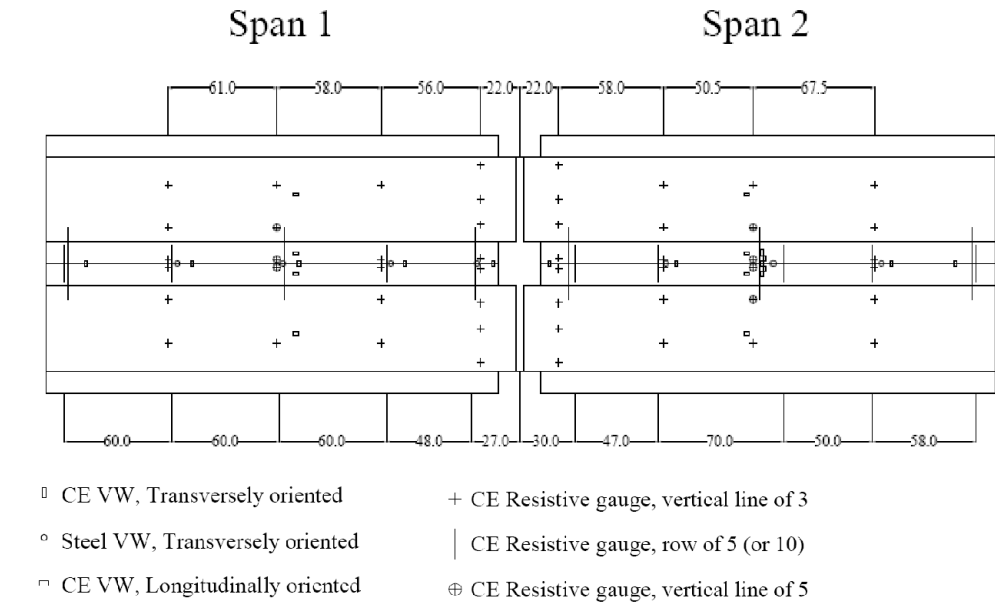

Figure 5 Instrumentation layout for Concept 1 laboratory bridge specimen (Smith et al. 2008).

consequence, the loads were subsequently increased to induce similar strains in the cross section as those observed in the Center City Bridge because of thermal effects. The figure shows the location of loads applied through a spreader beam to extend the reflective crack along the length of the joint.

In addition to the two large-scale laboratory bridge specimens, six subassemblage specimens were tested to investigate the relative performance of various reflective crack control reinforcement details. Figure 7 shows the elevation and plan views of a representative subassemblage specimen. Table 2 lists the variables investigated in each of the subassemblages. The reinforcement ratio for crack control, given in Table 2, considered the area of all reinforcement crossing the precast joint near the bottom of the CIP

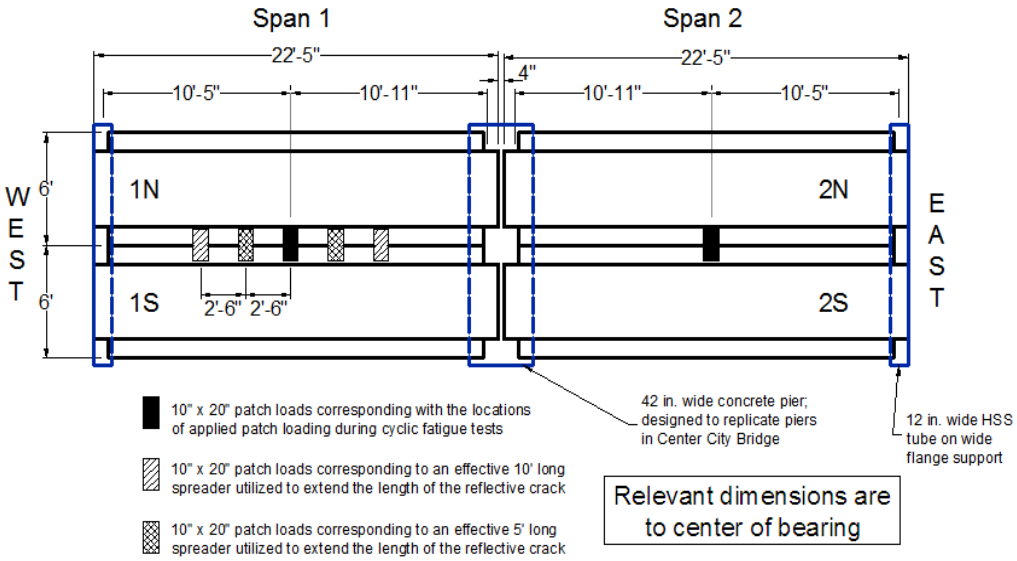

Figure 6 Placement of patch loads during fatigue loading and extension of longitudinal reflective cracking (applicable in Span 1 only) for the Concept 1 laboratory bridge specimen.

Copyright National Academy of Sciences. All rights reserved.

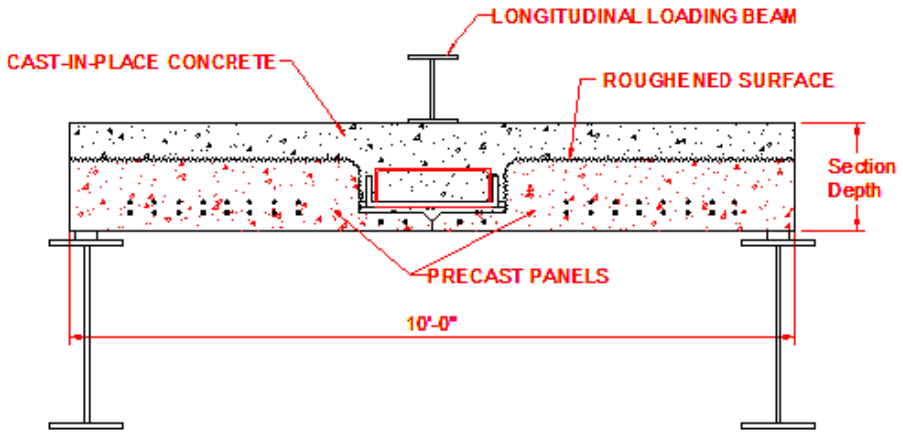

(a) Elevation view of subassemblage specimens

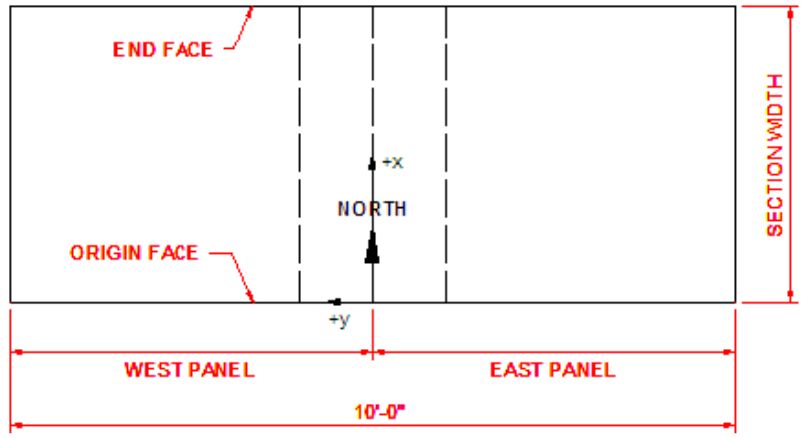

(b) Plan view and directional orientation of subassemblage specimens

Figure 7 Elevation and plan views of subassemblage specimen.

trough. Therefore, the bottom leg of the cage stirrups and all of the embedded transverse reinforcement were included in the calculation (i.e., for each pair of transverse embedded bars, both were included in the calculation because both were assumed to be effective above the longitudinal joint between the adjacent flanges). Furthermore, the area of concrete used in the calculation was only that which was located between the top of the precast flanges and the top of the precast webs. It should be noted that this crack control reinforcement would only be effective in the region above the longitudinal joint between adjacent precast panels. For potential cracks that may develop at the precast web-CIP interface, only the reinforcement protruding from the precast webs would be effective.

The specimens were loaded to flexurally induce cracking above the longitudinal joint between the precast flanges. The size, quantity, and location of cracking were documented through a range of quasi-static and cyclic load tests. Figure 8 illustrates the method for documenting the visual observations. The subassemblages were instrumented internally to investigate the location of the cracking along the depth and through the thickness of the structure. The results obtained from the internal instrumentation were compared to visual observations of crack initiation, width, and depth observed on the faces of the specimen.

Following the tests of the laboratory bridge and subassemblage specimens, a forensic examination of the specimens was conducted. Cores were taken in the region over the longitudinal joint between the adjacent precast flanges and above the CIP-precast web interface, as shown in Figure 9, to look for evidence of any residual reflective cracks under no loading.

Copyright National Academy of Sciences. All rights reserved.

Table 2 Subassemblage specimen design details.

Specimen ID	Width [in.]	Depth [in.]	Transverse Bars (Load Trans.)			Cage (Crack Control)			Max Spacing[2]	R/F Ratio
			Size	Spacing	Depth[1]	Presence	Size	Spacing		ρ_{cr}
SSMBLG1-Control1	62.75	14	#4	18 in. OC	4½ in.	Cage	#3	18 in. OC	9 in.	0.0031
SSMBLG2-NoCage	67.25	14	#4	18 in. OC	4½ in.	No Cage	0	0	18 in.	0.0025
SSMBLG3-HighBars	62.75	14	#4	18 in. OC	7 in.	Cage	#3	18 in. OC	9 in.	0.0031
SSMBLG4-Deep	62.75	18	#4	18 in. OC	4½ in.	Cage	#3	18 in. OC	9 in.	0.0022
SSMBLG5-No.6Bars	62.75	14	#6	18 in. OC	4½ in.	Cage	#3	18 in. OC	9 in.	0.0061
SSMBLG6-Frosch	64	14	#4	18 in. OC	4½ in.	Cage	#3	4.5 in. OC	4.5 in.	0.0052
SSMBLG7-Control2	62.75	14	#4	18 in. OC	4½ in.	Cage	#3	18 in. OC	9 in.	0.0031

[1]The depth of the transverse reinforcement was taken from the bottom of the precast section to the center of the reinforcement.
[2]The maximum spacing was the maximum nominal distance between reinforcement traversing the longitudinal joint, regardless of type (i.e., transverse hooked bars or cage).
NOTE: R/F ratio = reinforcement ratio, ρ_{cr} = reinforcement ratio for crack control, OC = on center.

There were a few considerations not included in the laboratory research or numerical study, such as the connection between the precast elements and the substructure. These details were investigated primarily by means of examination of structural plans for existing PCSSS structures.

Conclusions and Recommendations

The conclusions and recommendations are summarized by topic.

Bursting, Splitting and Spalling Stresses

Significant changes have been made to the bridge design specification since 2007 with regard to end zone stresses, specifically in the terminology. Up to and including the 2007 specifications, the term "bursting" was used to describe the end zone stresses and was associated with design requirements likely developed specifically for I-girders, but also applied to other shapes. The 2008 Interim specifications relaxed the placement requirements for wide-shallow

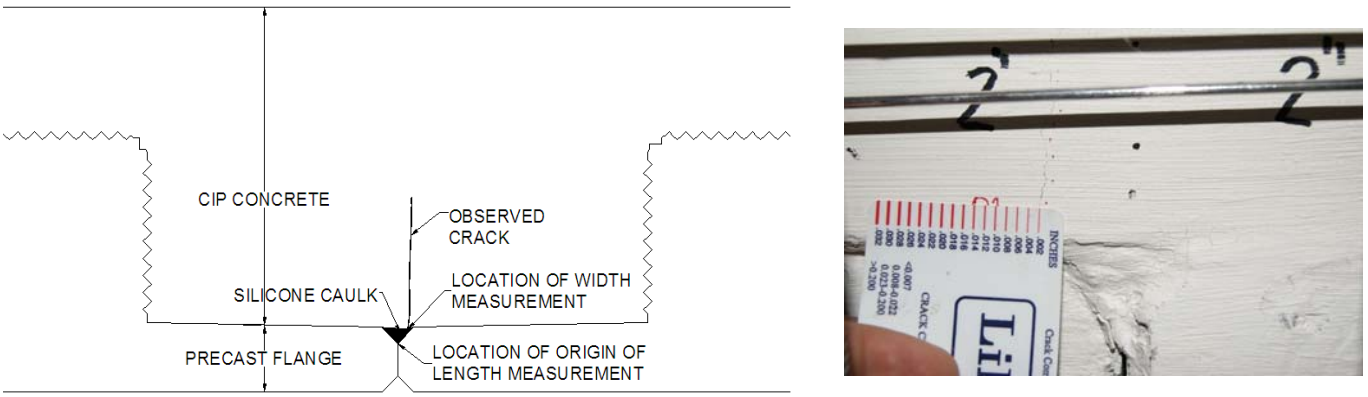

Figure 8 Measurement of width and length of crack observed on origin and end faces of subassemblage specimens.

Copyright National Academy of Sciences. All rights reserved.

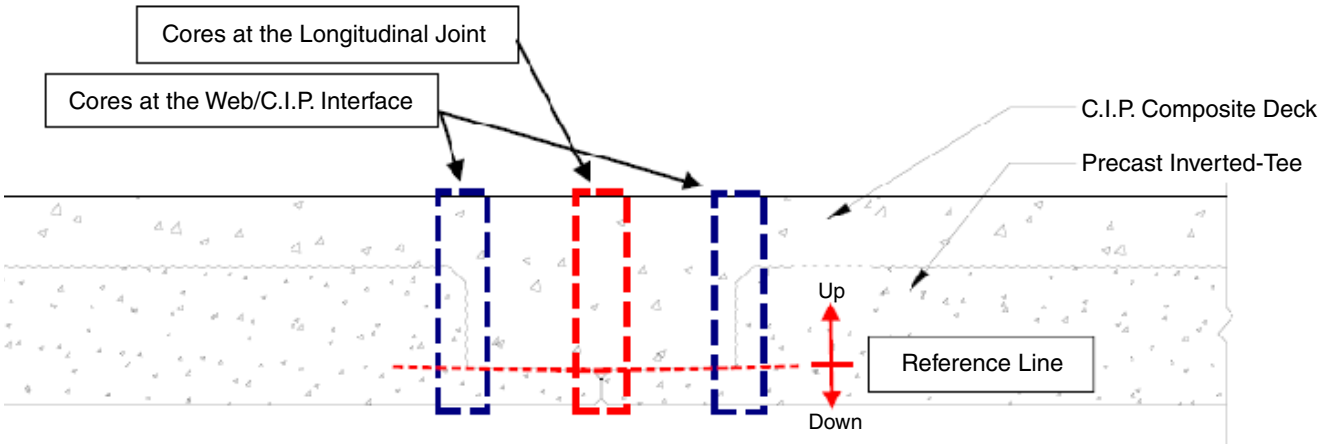

Figure 9 Location of cores removed from the test specimen and reference line for measurement of vertical location of cracking in subassemblage core specimens.

sections by allowing the designer to spread the end zone reinforcement, termed "splitting" reinforcement, over a larger distance. In the case of pretensioned solid or voided slabs, the designer can substitute the section width for "*h*," rather than using the section depth for "*h*." According to this study, this may not be appropriate when trying to control spalling stresses. In addition, the terminology for the reinforcement described in this section of the design specifications is more correctly termed "spalling" reinforcement rather than "splitting" or "bursting" reinforcement (Uijl 1983). Figure 10 illustrates the correct terminology to describe the end zone stresses in prestressed members.

Experimental and numerical studies were completed to investigate the effects of end zone stresses on the precast prestressed inverted-T sections used in the PCSSS. The experimental results from the Concept 1 and 2 laboratory bridge investigations indicated that the 12-in. deep concrete sections had sufficient strength to resist tensile stresses induced in the transfer zone of the precast inverted-T sections at the time of release. Four unique end regions of the Concept 1 laboratory bridge specimen precast members did not exhibit any evidence of cracking, even in the absence of vertical reinforcement. These findings were corroborated with the results of numerical studies.

Results from the finite element study (Eriksson 2008) revealed that the relationship between $e^2/(h * d_b)$ (where e stands for prestress eccentricity, h stands for section depth, and d_b stands for strand diameter) and

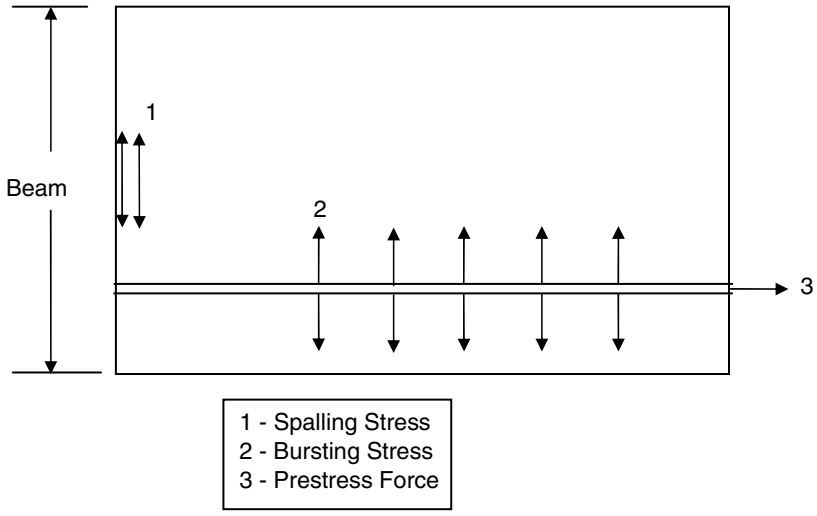

Figure 10 End zone stresses in prestressed members.

Copyright National Academy of Sciences. All rights reserved.

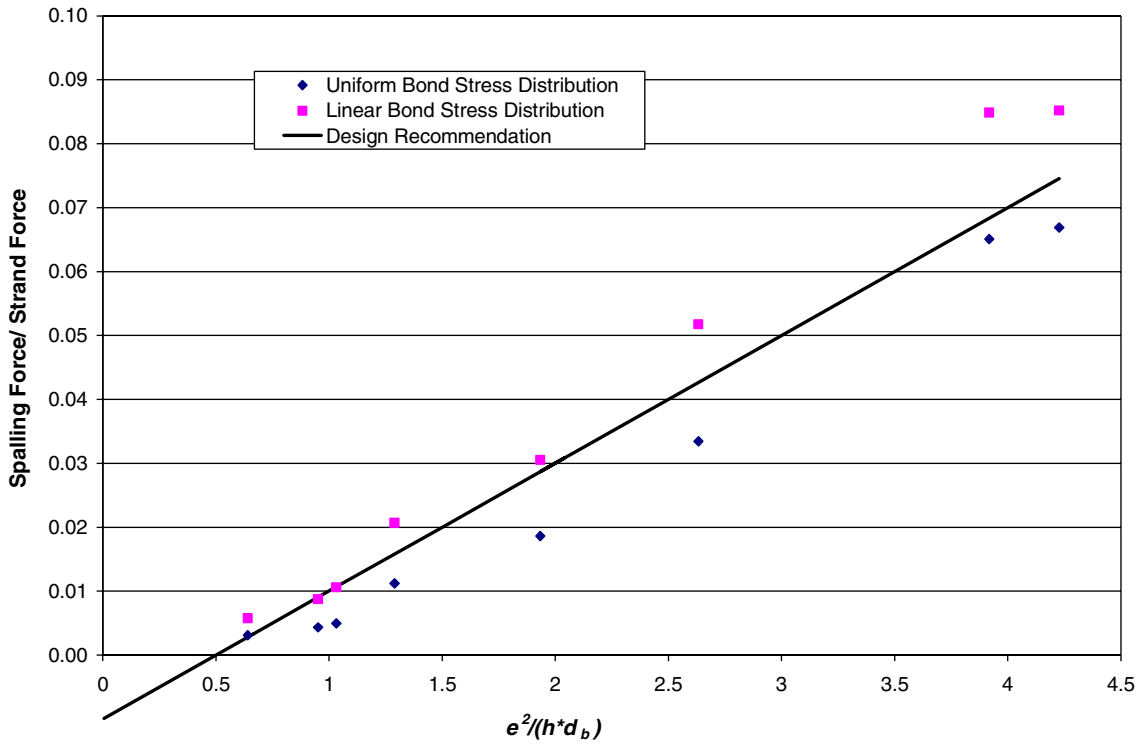

Figure 11 Ratio of spalling force to prestress force for varying $e^2/(h*d_b)$.

the ratio of tensile spalling force to prestress force is reasonably approximated by a straight line as shown in Figure 11. Because the true bond stress distribution is somewhere between uniform and linear bond stress, an average between these two assumptions was developed, as shown in Figure 11. The equation for this straight line approximation is

$$T = P\left(0.02\frac{e^2}{hd_b} - 0.01\right) \geq 0 \quad (1)$$

where T is the spalling force and P is the strand force.

Vertical steel reinforcement does not carry the vertical tensile stress until the concrete cracks. If the spalling stresses are small enough in a member for the concrete tensile strength to prevent cracking, vertical tensile steel is not necessary for the member.

To calculate the concrete area to be considered for providing tensile resistance, the area over which spalling forces act must be determined. Based on the slab span sections studied, the shortest distance into the member the spalling stress extends is $h/12$. This becomes a conservative estimate as the section increases in height and e/h. The area of concrete to resist this tensile strength is conservatively estimated as the product between $h/12$ and the distance between the outermost prestress strands (b_s) and can be written as

$$T_c = 0.24\sqrt{f_c}\frac{h}{12}b_s \quad (2)$$

where T_c is the tensile force that can be resisted by the concrete, f_c is the concrete compressive strength at 28 days, h is the height of the member (the precast slab), and b_s is the distance between the outermost pretension strands. If the design tensile force is smaller than the tensile force resisted by concrete ($T < T_c$), it is reasonable to assume cracking will not occur and vertical tensile steel is not needed in the end region to resist the spalling force. Otherwise, steel must be placed within the end region of the member to resist the tensile force found in Equation (1). The area of steel needed to resist the predicted spalling force is given by

$$A_s = \frac{T}{f_s} \quad (3)$$

where A_s is the area of steel and f_s is the allowable working stress of vertical reinforcement.

Copyright National Academy of Sciences. All rights reserved.

The numerical studies showed that certain inverted-T members did not require spalling reinforcement, specifically those with depths less than 22 in. for which the expected concrete tensile strength was larger than the expected vertical tensile stresses due to the development of prestress.

It was also found through numerical studies that the existing design requirements may not be conservative for deep inverted-T sections (i.e., greater than 22 in.). Larger amounts of spalling reinforcement than specified by the 2010 design specifications were found to be required. It was also found that the reinforcement should be placed as close to the end of the member as possible (i.e., within *h*/4 of the end of the member, where "*h*" represents the depth of the member). The end region was the most critical region for the reinforcement to be located to address spalling stresses, even for the case of wide sections.

Restraint Moment

Multispan precast composite bridge structures made continuous with CIP concrete develop time-dependent and thermal restraint moments at the continuous piers. The size and magnitude of restraint moments are affected by shrinkage, creep, age of the precast members at the time of continuity, and thermal gradients. Positive and negative restraint moments are illustrated in Figure 12.

Negative restraint moments are caused by differential shrinkage of the CIP concrete, where the rate of shrinkage of the CIP concrete is larger than the rate of shrinkage and creep of the precast member. When the precast member is at a relatively old age, defined as greater than 90 days by AASHTO, the shrinkage of the newly placed CIP concrete will tend to "shorten" the top fiber of the bridge structure and subsequently induce longitudinal tensile stresses in the top of the bridge at the piers. The reinforcement included in the deck of the structure over the piers in continuous systems provides the tension ties necessary to counteract negative restraint moments.

Positive restraint moments at the piers in continuous systems may be due to both time-dependent and thermal effects. When the precast member is at a relatively young age at the time of continuity, the rate of shrinkage of the precast member and the CIP may be similar; however, the precast member would also undergo creep. The creep of the precast section would tend to "shorten" the bottom fiber of the bridge structure and subsequently induce longitudinal tensile

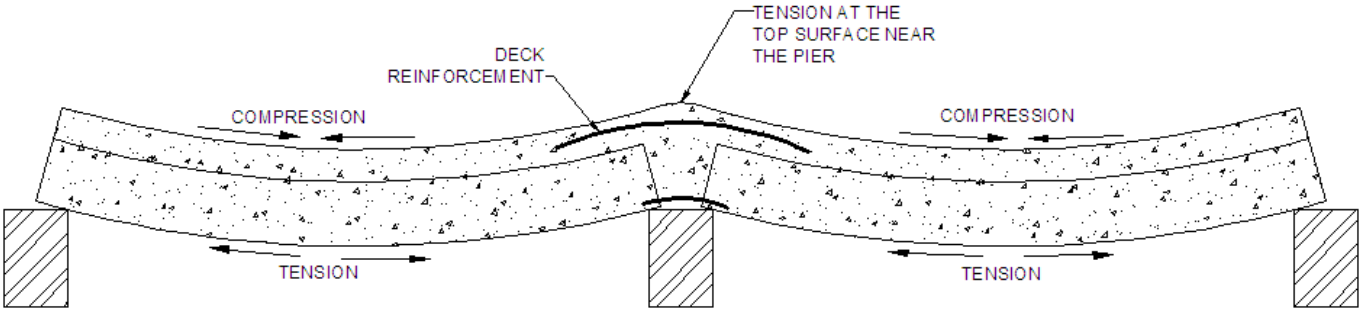

Negative restraint moment induces tension near the top surface at the pier.

(a)

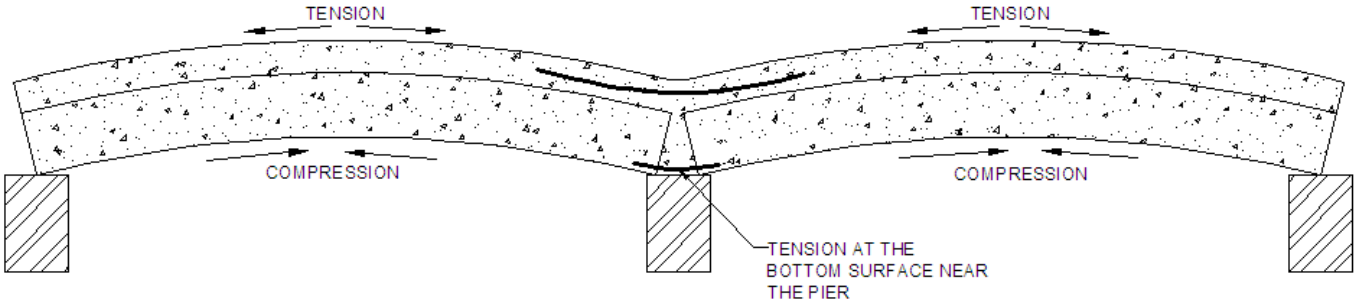

Positive restraint moment induces tension near the bottom surface at the pier.

(b)

Figure 12 Positive and negative restraint moments in continuous bridge superstructures (Molnau and Dimaculangan 2007).

Copyright National Academy of Sciences. All rights reserved.

stresses in the bottom of the bridge at the pier. In addition, thermal gradients in the section cause the top surface of the structure to expand, again inducing a positive restraint moment in the structure. For this reason, both time-dependent and thermal gradient effects must be considered in the design of positive restraint moments. Because positive restraint moments induce longitudinal tensile stresses near the bottom of the section, reinforcement must be provided to carry the tensile force at the piers. Because of the sectional geometry of the PCSSS, all reinforcement provided for positive restraint moments must be located within the longitudinal trough regions between precast panels. Consequently, this reinforcement must be placed in groups centered between panels, generally 6 feet apart, thereby prohibiting the distribution of the reinforcement along the face of the bottom surface.

Research completed during the Mn/DOT study and the current study has shown that restraint moments that develop due to thermal gradients can be significant and should be considered in either case (i.e., whether or not time-dependent effects generate positive or negative restraint moments). The positive restraint moment effects attributed to the design thermal gradients can be an order of magnitude larger in some climates than the positive restraint moments due to time-dependent effects. The thermal gradients provided by the bridge design specification should be taken into consideration by calculating the resulting expected curvatures of each span treated as simply supported and then determining the moment required to overcome the end rotations and provide continuity. There may be little or no economic gain in continuity because of the large thermal restraint moments that develop and, in some cases, continuity may require additional reinforcement in the precast sections (i.e., larger than would be required for a simply-supported design). As a consequence, it is not conservative to design the PCSSS bridges as simply supported and add positive moment reinforcement across the piers for integrity reinforcement without considering the effects of the restraint moments that can be generated due to the thermal gradient effects.

Live Load Distribution Factors

Numerical modeling was combined with observations from a live load truck test on the field-instrumented Center City Bridge along with load distribution tests on the laboratory bridge specimens (i.e., Concept 1 and Concept 2) to determine the applicability of current live load distribution factors in the bridge design specification for slab-type bridges to the PCSSS.

The numerical models illustrated that the longitudinal curvatures measured in the precast slab span system with a reflective crack extending to within 3 in. of the extreme compression fiber and a tandem load greater than that which could be physically applied in the field resulted in longitudinal curvatures that were only 84% of the longitudinal curvatures predicted using the AASHTO Load and Resistance Factor Design (LRFD) (2010) load distribution factors for monolithic concrete slab span bridges. This suggests that PCSSS-type superstructures could reasonably and conservatively be designed using the current live load distribution factors for monolithic slab-type bridges.

Furthermore, the live load truck tests on the Center City Bridge suggested that the measured longitudinal curvatures were approximately three times less than those calculated using monolithic slab span equations. And the measured longitudinal curvatures were consistently conservative when compared to monolithic slab span finite element (FE) models. The conservatism in the factors for monolithic slab span bridges was sufficient to cover the cases of the PCSSS bridges even considering the potential effects of reflective cracking as discussed above.

Load distribution tests on Span 2 of the Concept 1 and Concept 2 laboratory bridges included an investigation of the transverse load distribution between adjacent precast panels. Both spans showed good load transfer capabilities across the longitudinal joint during intermittent tests to extend the reflective crack, conducted throughout the investigation of the laboratory bridge specimens. In both cases, little variation in the measured longitudinal curvatures with crack growth was observed in the unloaded panels, which suggested that load was effectively transferred across the longitudinal joint from the loaded panel despite the presence and increase in the size of reflective cracking induced in/near the joint.

In summary, the numerical and experimental studies in regards to live load distribution factors indicated that the PCSSS was well represented by monolithic FEM models, suggesting that the discontinuity at the precast joint did not significantly affect the load distribution characteristics of the system. Also, the performance of the large-scale laboratory

Copyright National Academy of Sciences. All rights reserved.

bridge specimens reinforced the notion that the system provided sufficient transverse load distribution, with and without the presence of reflective cracking near the joint region.

Skew

Numerical modeling was applied to simply supported monolithic and jointed (to simulate the PCSSS discontinuity at the adjacent precast flange interface) bridge models with skewed supports ranging up to 45 degrees. Three independent load cases were investigated, including a 35-kip load individually applied over a 12- by 12-in. patch at both quarter points and at midspan for each model. For each load case, the largest horizontal shear stress in the plane above the precast joint nearest the loading was determined. The small variation and consistency between the models considering a joint between precast sections with a 3-in. flange and a monolithic structure suggested that the impact of the joint in precast composite slab span construction was not expected to significantly affect the performance of the system in skewed applications, and the design of skewed PCSSS bridges could be completed assuming a monolithic slab span system.

Composite Action and Horizontal Shear Strength

To conclude the laboratory tests, the large-scale bridge specimens were loaded above the nominal flexural capacities to the limiting capacities of the actuators in order to investigate the ability for the precast slab span sections to remain composite with the CIP concrete topping. Placement of reinforcement for horizontal shear was observed to be difficult and time consuming for the fabricator, especially when finishing the top web surfaces. Furthermore, the reinforcement extending from the precast webs for horizontal shear extended out of the precast section with minimal clearance between the hook and the precast web surface in order to avoid interference with placement of the deck reinforcement in the field. In initial field applications of the PCSSS, the low clearance of this horizontal shear reinforcement may have limited its effectiveness because aggregate was unable to flow below the returned stirrups. Span 2 of the Concept 2 laboratory bridge was designed with the same horizontal shear layout utilized in the Center City Bridge, which satisfied the 2005 bridge design requirements. Span 1 of the Concept 1 laboratory bridge was designed with fewer horizontal shear ties than were used in Span 2 and in the Center City Bridge, which did not satisfy the minimum horizontal shear reinforcement requirements of the 2005 bridge design requirements. The Concept 2 laboratory bridge was designed and constructed with no horizontal shear ties. In both bridges, the surface condition of the precast member was roughened to a surface consistent with a ¼-in. rake.

In the tests on both spans of the Concept 1 laboratory bridge and on the Concept 2 laboratory bridge, the sections were observed to remain composite well beyond service load levels through the full range of loading to the maximum capacity of the loading system, which was in excess of the predicted nominal capacity of the Concept 1 and 2 bridges. The horizontal shear stress estimated in the Concept 2 system at the precast-CIP interface was subsequently calculated to be 135 psi. As the bridge had not yet been loaded to failure due to the limited capacity of the actuators, it may have been possible to generate even larger horizontal shear stresses.

The results of the laboratory tests are consistent with those of Naito and Deschenes (2006) and suggest that the bridge design specification should allow for the design of precast slab span structures without horizontal shear ties, and allow for the development of a maximum factored horizontal shear stress of 135 psi in sections with intentionally roughened surfaces (i.e., ¼-in. rake as shown in Figure 13 for the Concept 2 bridge) unreinforced for horizontal shear.

Reflective Crack Control across the Longitudinal Joint between Precast Flanges

Reflective cracking was intentionally induced in the Concept 1 and Concept 2 large-scale laboratory specimens to investigate the performance of the PCSSS through a range of loading that was designed to simulate both fatigue performance due to vehicular loading as well as the influence of environmental effects. The performance of both spans of the Concept 1 laboratory bridge and the Concept 2 laboratory bridge was observed to adequately control cracking in the precast joint region throughout the loading.

Reflective cracking was also monitored throughout the range of testing for seven subassemblage specimens in order to quantify the relative performance of the respective design details for reflective crack control in each specimen. The ability for each specimen to control the width of cracking was

Copyright National Academy of Sciences. All rights reserved.

Figure 13 Intentionally roughened surface, by means of raking, of top web of precast beam used for the construction of Concept 2 laboratory bridge specimen.

desirable, as large cracks were expected to cause degradation of the longitudinal joint region. This degradation included providing a potential avenue for the ingress of moisture and chlorides.

It was found during the testing of the first specimen, SSMBLG3-HighBars, that the stiff flanges of the precast section rotated and caused delamination between the precast flange and CIP concrete, resulting in propagation of a crack at the precast-CIP concrete interface. The test setup was subsequently modified by developing a system to clamp the precast flanges to the CIP concrete on either side of the longitudinal joint as shown in Figure 14. Although the test setup induced compressive forces through the depth of the section at the faces, it was believed to better emulate the field conditions because in a bridge system, the pier supports would be normal to the longitudinal joint, thereby preventing the relative rotation of the precast flanges with respect to the CIP in the trough above the precast flanges at the ends of the sections.

The vertical rods that connected the top and bottom steel members used to clamp the section were located a clear distance of between 2 in. and 3 in. from the face of the specimen. Consequently, curvature was induced in the longitudinal clamping members, which tended to concentrate the compressive force at the ends of the members. This served to better simulate the effects of restraint in the bridge system (i.e., clamping the subassemblage specimens near the ends simulated the effect of the bridge supports transverse to the longitudinal joint and relieved the compressive stress across the subassemblage).

Each of the subassemblage specimens performed adequately throughout the range of loading, though variations in the extent of cracking indicated some relative differences. The two specimens with the largest reinforcement ratios for crack control, SSMBLG5-No.6Bars (ρ_{cr} = 0.0061) and SSMBLG6-Frosch (ρ_{cr} = 0.0052), performed well relative to the remaining specimens. In these two specimens, measured crack widths were consistently smaller than the remaining specimens. SSMBLG7-Control2 (ρ_{cr} = 0.0031) also indicated better than average performance through visual observations, however, the analysis of the embedded instrumentation suggested that the behavior of this specimen was similar to the specimens in the group not including SSMBLG5-No.6Bars and SSMBLG6-Frosch. The behavior of SSMBLG7-Control2 was attributed to a relatively smooth precast flange surface achieved prior to the placement of the CIP concrete (done in anticipation of studying a debonded flange surface, which was abandoned to allow for a second control specimen

Copyright National Academy of Sciences. All rights reserved.

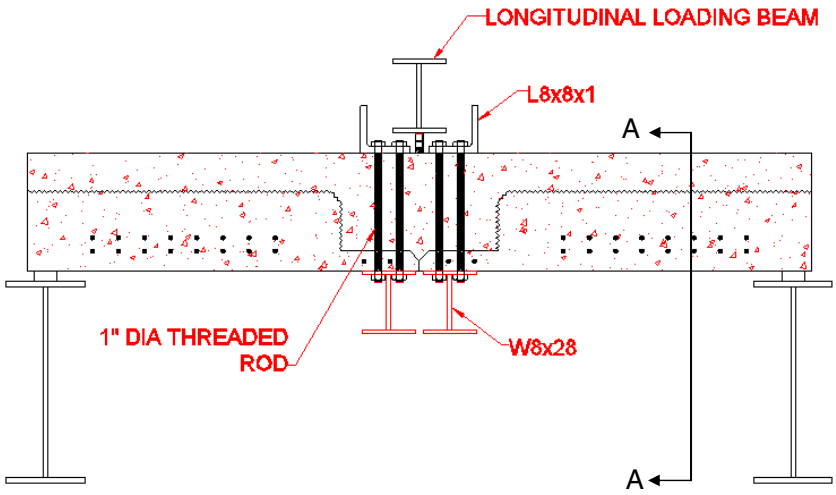

Figure 14 Clamping system developed to simulate restraint near joint region on subassemblage specimens.

to be tested). The relatively smooth flange surface was expected to better distribute transverse stresses across the precast flanges in the joint region, thereby reducing the potential stress concentration at the interface between the adjacent precast flanges that created a longitudinal joint. However, it was observed via an analysis of the horizontal crack propagation using the concrete embedment resistive strain gages that a single crack was present internally in the specimen suggesting that the smooth flange surface did not distribute the transverse stress adequately enough so as to promote the development of multiple cracks. A completely debonded surface, however, was not expected to be desirable as it would likely promote delamination of the horizontal precast flange-CIP interface, which was expected to promote cracking at the vertical precast web where cage reinforcement was not present to aid in the control of cracking.

In the subassemblage study, the maximum transverse 9-in. spacing for crack control appeared to be sufficient as long as enough reinforcement was provided to ensure that the reinforcement did not yield upon cracking. This was evident through the good performance of the SSMBLG5-No.6Bars and SSMBLG6-Frosch specimens. These results are consistent with those of Frosch et al. (2006).

The maximum transverse reinforcement spacing was further investigated by evaluating the performance of the Concept 1 and 2 laboratory bridges, which provided more realistic boundary conditions in the longitudinal joint region above the precast flanges. In this study, it was found that the 9-in. maximum transverse reinforcement spacing provided in the Concept 2 laboratory bridge did not correlate with an improvement in the control of cracking near the longitudinal trough area relative to the 12-in. maximum spacing provided in the Concept 1 spans. Therefore, an economical design may favor 12-in. transverse reinforcement spacing to 9-in. spacing with no expected reduction in performance. An increase in the maximum transverse reinforcement spacing to 18 in. is not recommended, primarily because cracking in SSMBLG2-NoCage (which was reinforced with only transverse No. 4 bars spaced at 18 in.) was generally largest. The crack widths in SSMBLG2-NoCage increased with the least increase in the applied load relative to the other subassemblage specimens that had transverse reinforcement spacings no larger than 9 in. The subassemblage specimen with transverse reinforcement spacing no larger than 9 in. were observed to provide acceptable crack control.

Furthermore, little difference was observed between the performance of the sections of the Concept 1 laboratory bridge with No. 6 transverse hooked bars where reflective cracking was observed and the performance of the Concept 2 laboratory bridge with No. 4 transverse hooked bars where reflective cracking was observed. There was, however, a noticeable increase in the relative performance of SSMBLG5-No.6Bars compared to SSMBLG1-Control1, in which the only nominal difference was the larger bars in the former specimen. Because the increased performance observed in SSMBLG5-No.6Bars,

Copyright National Academy of Sciences. All rights reserved.

which performed similar to SSMBLG6-Frosch, was achieved with larger bars and a maximum transverse reinforcement spacing of 9 in., it was suggested that a design with No. 6 bars and less cage reinforcement was likely to be more economical and easier to implement in the field than the closely spaced reinforcement cage provided in SSMBLG6-Frosch, which had a 4.5-in. bar spacing.

Design Recommendations and Examples

Recommended changes to the bridge design and construction specifications were proposed to implement this promising new system. The PCSSS bridge design guidelines cover both component and system issues, including "spalling" reinforcement, load distribution, effect of restraint moments, composite action, and reinforcement to control reflective cracking. Two MathCAD examples were created to illustrate the design issues associated with a simply supported PCSSS and a three-span system made continuous. Because of the effects of thermal gradients in generating large restraint moments, it is suggested that the PCSSS bridges be designed as a series of simply supported spans.

LONGITUDINAL AND TRANSVERSE JOINTS IN DBT AND FULL-DEPTH PRECAST PANEL ON GIRDER SYSTEMS

Introduction

Two issues that limited the PCSSS bridge concept with regard to the potential for accelerated bridge construction applications were (1) the significant use of CIP to complete the composite system, which would slow the construction process and (2) the limitation of the system to short- to moderate-span lengths. As a consequence, the study included CIP connection concepts that minimized the use of CIP by limiting its application to the longitudinal and transverse joints between the flanges of DBTs or between full-depth precast deck panels on girders. Because of the similarity in these systems, the discussion herein focuses primarily on DBTs, which generally have greater constraints on deck thickness than precast panel systems.

The bridge deck in DBTs consists of the girder flange, which is precast and prestressed with the girder. DBTs are manufactured in the precast plant under closely monitored conditions, transported to the construction site, and erected such that the flanges of adjacent units abut. Load transfer between adjacent units is provided by longitudinal joints (parallel to traffic direction). Figure 15 shows a DBT bridge being constructed.

The DBT bridge system eliminates the time necessary to form, place, and cure a concrete deck at the bridge site. In addition, the wide top flange provided by the deck improves construction safety due to ease of installation, enhances durability because the deck is fabricated with the girder in a controlled environment, and enhances structural performance with a more efficient contribution of the deck in stress distribution. Despite the major benefits of this type of bridge, use has been limited to isolated regions of the United States because of concerns about certain design and construction issues. This project aimed to address one of the hurdles to be overcome to enable a wider use of this technology: the development of design guidelines and standard details for the joints used in these systems. The aim of the study was to produce full strength durable joints using CIP, but still allow for accelerated construction.

Figure 16 shows a typical DBT bridge consisting of five DBTs connected by four longitudinal joints with welded steel connectors and grouted shear keys (Stanton and Mattock 1986; Ma et al. 2007). In order to reduce the total DBT weight, the thickness of the deck is typically limited to 6 in. Welded steel connectors are typically spaced at 4 ft. To make the connection, as shown in Figure 16, two steel angles are anchored into the top flange of the DBT and a steel plate is welded to steel angles in the field. Between two connectors, a shear key is provided at the vertical edge of the top flange. Grout is filled into the pocket of the connector and in the voids of the shear

Figure 15 A DBT concrete bridge being constructed.

Copyright National Academy of Sciences. All rights reserved.

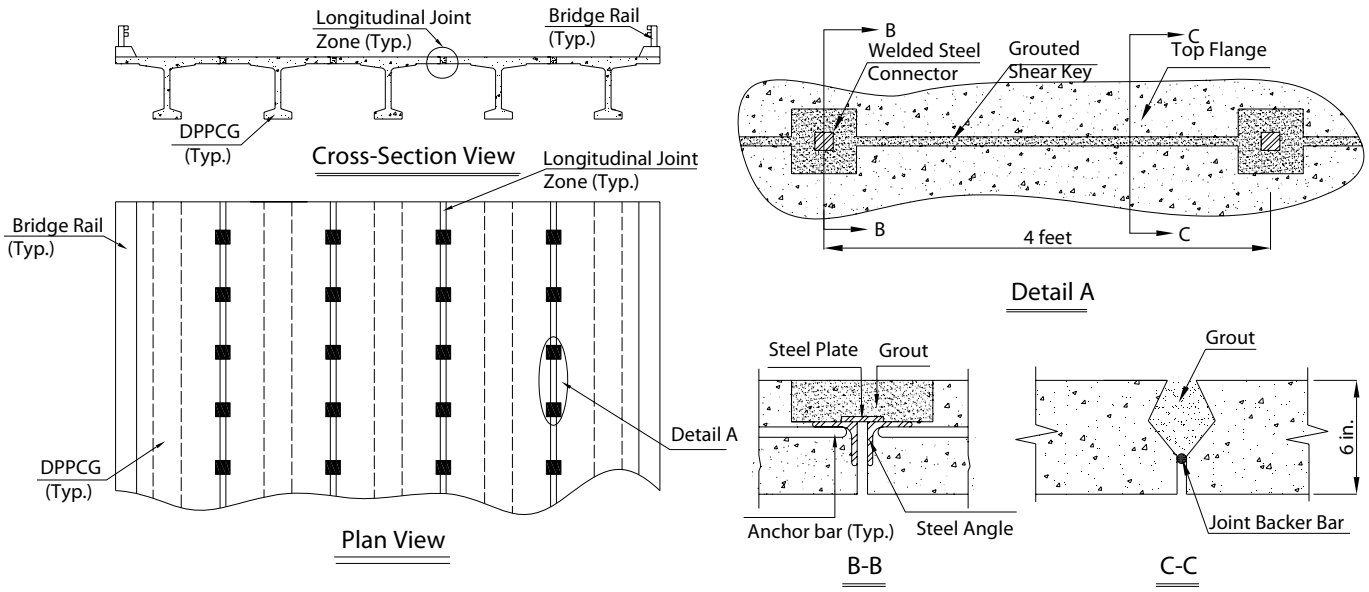

Figure 16 A typical DBT bridge connected by longitudinal joints with welded steel connectors. (Typ = typical, DPPCG = decked precast, prestressed concrete girder bridges, B-B and C-C = cross sections defined in Detail A.)

key to tie the adjacent girders together. A joint backer bar is placed at the bottom of the shear key to prevent leakage when grouting.

The typical longitudinal joint shown in Figure 16 has the strength needed to transfer shear and limited moment from one girder to adjacent girders. The width of the joint zone is small so that it facilitates accelerated construction. However, because the welded steel plates are located 4 ft from each other and at mid-depth of the flange, they cannot help to control flexural cracks along the longitudinal joint. Although the performance of this type of joint was reported as good to excellent in a survey of current users, problems with joint cracking in these systems have been reported in the literature (Stanton and Mattock 1986; Martin and Osborn 1983). This joint cracking along with joint leakage is perceived to be an issue limiting wider use of this type of bridge. The State of Washington limited the use of DBTs for roads with high average daily traffic (ADT) and for continuous bridges. As part of a research project to address issues that influence the performance of DBT bridges, a specific objective was defined to develop improved joint details that allow DBT bridge systems to be more accepted as a viable system for accelerated bridge construction.

One of the connection concepts explored was to replace the current welded steel connectors with distributed reinforcement to provide moment transfer as well as shear transfer across the joint. Well-distributed reinforcement can control cracks much better than widely spaced welded steel connectors. However, straight lap-spliced reinforcement requires a much wider joint to develop its strength. It is very important for the proposed joint width to be as narrow as possible. Joint width minimization will reduce the amount of required expensive grout, which results in a reduction of cost and faster construction time. As a result, options to reduce the joint width were explored. Such options included bars with hooks (U-bar), bars with headed terminations, and bars with spirals. To allow for accelerated construction, the details were also developed to minimize deck thickness, which would reduce the weight of DBT girders.

In total, five different connection concepts were proposed and evaluated for the longitudinal and/or transverse connections between full-depth deck panels or deck flanges for this study. Feedback on the details was obtained through an in-depth phone survey that included 60 participants. The respondents included bridge engineers (including many individuals who serve as State Bridge Engineers), consulting engineers, fabricators, material suppliers, industry representatives, and technical committee contacts. The five connection concepts that were addressed were loop bar (U-bar) detail, straight bar detail with spiral to reduce lap length, headed bar detail, welded wire reinforcement (WWR) detail, and structural tube detail.

In general, many respondents considered all five of the connection concepts to be potentially useful

Copyright National Academy of Sciences. All rights reserved.

in bridge construction and especially when rapid construction was critical. A common concern regarding the connection of each of the precast elements was that of differential camber, and many respondents who voiced this concern suggested that the use of a steel plate or haunch should be included to assist with the leveling of adjacent precast panels.

Many of the respondents preferred the U-bar detail over the other options and noted that a U-bar detail has been successful in Japan and Korea. Some expressed that although the U-bar detail was the most promising, it could require a thicker deck to accommodate the bend radius of the U-bar detail, which would add weight to the structure. It was suggested by another that the key to the U-bar detail would be to obtain a waiver on the minimum bend radius of the looped bar. Experience of a similar detail used in Nebraska indicated exceptional performance of the system; it was emphasized that the connection must be either nonshrink or expansive to prevent cracking. Some respondents commented that the U-bar detail would require perforations in the formwork, and therefore, the bar spacing should be standardized as much as possible.

The straight bar with spiral reinforcement to reduce the lap length detail was also favored by many of the respondents. A common concern regarding the connection was that it was expected to be more expensive and would also require additional field labor to complete the connection. In addition, it was suggested that the spiral reinforcement may create alignment issues during construction, which could add to the amount of construction time required.

The headed bar detail was often praised for the fact that it would come to the field site nearly completed, which would reduce construction labor as well as the time required to construct the system. Many respondents conceded little experience with the headed bar details and suggested that testing would be required, though many said that they expected that the detail would work adequately. Some respondents also suggested that the detail may be difficult to fabricate and that the alignment and placement of the longitudinal steel could be complicated.

The WWR detail was generally liked by most of the respondents, especially because the wire reinforcement detail was expected to promote rapid construction in the field. A few respondents voiced concern regarding the ability for the WWR to be adequately developed in the space available. In California, it was noted that WWR was not permitted, maybe due to a fatigue concern, though manufacturers are promoting its use.

Many of the respondents viewed the structural tube detail as being exceptionally robust, with one respondent describing it as being "bomb proof." A common concern regarding the structural tube detail was the potential for alignment and other constructability issues. Also of concern was the potential for sloppy field work to degrade the connection, especially if the tube were not correctly and completely filled with grout.

To finalize the connection concepts investigated in the study, the following criteria were considered:

- The connection detail should not only be able to transfer shear but also provide moment continuity across the joint. Where possible, two layers of steel should be used in the joint.
- The connection detail must allow the precast units to be joined together quickly to minimize disruption to traffic. For the joint connections, it is desirable to minimize or eliminate forming of the joint to expedite construction and reduce cost. Field placement of reinforcement within the longitudinal joint area after erection should be minimized. In joints where forming is required, provide sufficient room to facilitate connection completion and use CIP rather than special grout mixes.
- The closure pour (CP) material to precast unit interface is an area of concern for durability. The focus in this area must be on minimizing cracking in this location to reduce intrusion of water that may result in corrosion. Place the reinforcement as close as possible to the top and bottom surfaces to help control cracking.
- Cumulative fabrication and erection tolerances, particularly differential camber in deck flanges, will result in some degree of vertical flange mismatching. A temporary welded connector detail should be considered for leveling flange mismatching before the permanent connection is placed.

The U-bar detail and the headed bar detail were selected as the most viable candidates in this research. U-bar details are oriented vertically in the joint to provide two layers of reinforcement fabricated with a single rebar. The U-bars provide continuity of the deck reinforcement across the joint by lapping with the U-bars from the adjacent flanges. The 180° bend of the U-bar, embedded in the joint,

Copyright National Academy of Sciences. All rights reserved.

provides mechanical anchorage to the detail necessary to minimize the required lap length. The extended reinforcement of the U-bar details is staggered (i.e., out of phase) with the adjacent lapped U-bar to facilitate constructability in the field. The stagger cannot be too large, or the transfer of forces across the joint would be difficult to achieve.

To minimize deck thickness, the U-bar detail was designed to utilize an extremely tight bend. The inside bend diameter that was used was three times the diameter of the bar ($3d_b$), thus, with No. 5 bars used, the inside diameter of the bend was 1⅞ in. The American Concrete Institute (ACI) Committee 318-08 (2008) set minimum bend diameters for different rebar sizes and materials. For a No. 5 bar made of conventional steel, the minimum bend diameter, per ACI 318-08 (2008), was six times the diameter of the bar ($6d_b$), and for D31 deformed wire reinforcement (DWR) the minimum bend diameter was four times the diameter of the bar ($4d_b$) when used as stirrups or ties. Clearly, the U-bar bend diameter that was used ($3d_b$) violated the minimum allowable bend diameters established by ACI 318-08 (2008). The minimum bend diameters were established primarily for two reasons: feasibility of bending the reinforcement without breaking it and possible crushing of the concrete within the tight bend. To ensure that the reinforcement would not be broken while bending, two ductile reinforcing materials were used: DWR and stainless steel (SS) reinforcement. Concrete crushing in the tight bend was closely observed in the experimental investigation to determine if it would occur.

As an alternative to the U-bar details, two layers of headed bars were considered to provide continuity of the top and bottom deck steel through the joint. The previous NCHRP Project 12-69 explored the use of single large-headed bars to provide continuity across the joint (Oesterle et al. 2009; Li et al. 2010; Li et al. 2010a). In that project, Headed Reinforcement Corporation (HRC) provided the headed reinforcement, which consisted of a No. 5 bar with a standard 2-in. diameter circular friction welded head with a head thickness of 0.5 in. Large-headed bars such as these with the bearing area (A_{brg}), exceeding nine times the area of the bar (A_b), are assumed to be able to develop the bar force through bearing at the head. Bars with smaller heads (e.g., $A_{brg}/A_b \geq 4$) are assumed to be able to develop the force in the bar through a combination of mechanical anchorage and bond, where the development length for these bars is less than that required to develop a hooked bar per ACI 318-08 (2008). In the current study, the headed reinforcement used was No. 5 bar with Lenton Terminator® bearing heads. The diameter of the head was 1.5 in., and the thickness of the head was ⅞ in., which gave an A_{brg}/A_b of 4.76. The smaller head dimension was necessary in order to fit the two layers of reinforcement within the deck while minimizing the deck thickness. The large-headed bars in two layers would have resulted in a much thicker, uneconomical deck system.

In addition to the reinforcement details used for the connection, a key to the success of robust accelerated construction is the development of durable fast-curing CP materials. As a consequence, this investigation included the development of performance specifications to address the durability issues associated with the CP materials. Both overnight cure and 7-day cure materials were evaluated.

Research Methodology and Findings

Determination of Most Viable Connection Detail

Experimental tests were conducted on the selected reinforcement details to simulate the expected loading conditions to be experienced in longitudinal and transverse joint configurations. The investigated joints used two layers of reinforcement to provide the ability to transfer moment as well as shear through the deck. The two types of details investigated to reduce the width of the joint were U-bar details (with DWR and SS) and headed reinforcement details.

Initial tests were conducted using monolithic specimens that contained the two types of reinforcement details to simulate longitudinal and transverse joint connection concepts (i.e., flexural and tension test specimens, respectively). Both joint directions were investigated so that the results of this experimental program could apply to several precast deck systems (e.g., DBT systems and full-depth precast deck systems). Figure 17 shows the two joint directions tested and the specimen orientations used to represent the joints. The test setups for the longitudinal joint test (i.e., flexural test setup) and transverse joint test (i.e., tension test setup) are given in Figures 18 and 19, respectively.

Three of the specimens represented longitudinal joint connections (flexural specimens) and three represented transverse joint connections (tension

Copyright National Academy of Sciences. All rights reserved.

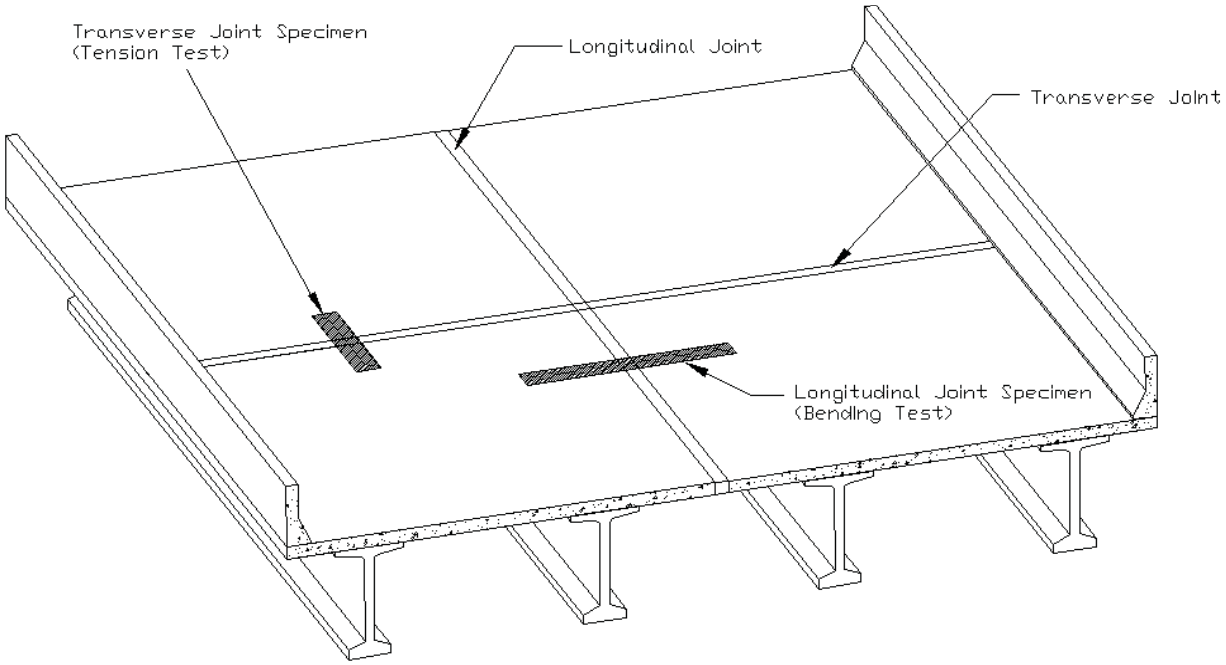

Figure 17 Orientation of joints and corresponding test specimens.

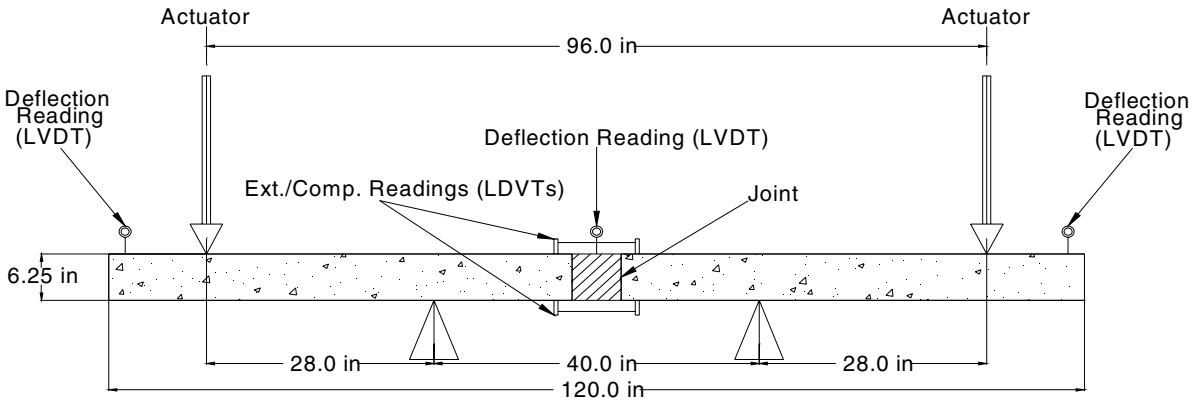

Figure 18 Flexural test set-up (longitudinal joint test) (LVDT = linear variable differential transformer).

Copyright National Academy of Sciences. All rights reserved.

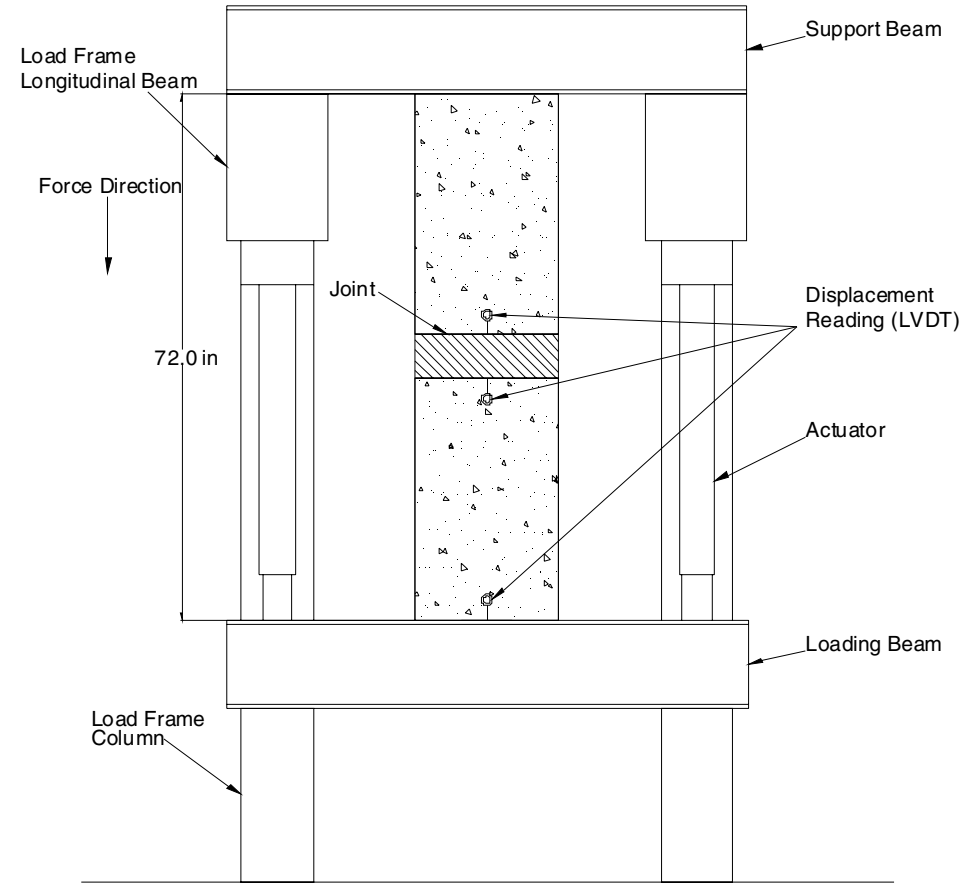

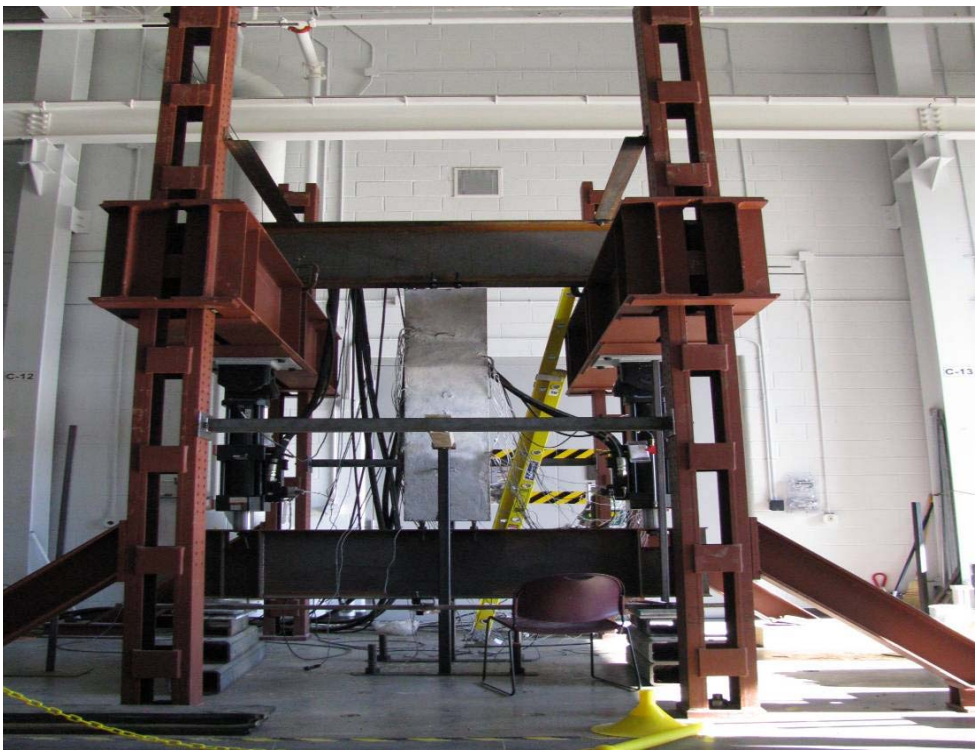

Figure 19 Tension test setup (transverse joint).

Copyright National Academy of Sciences. All rights reserved.

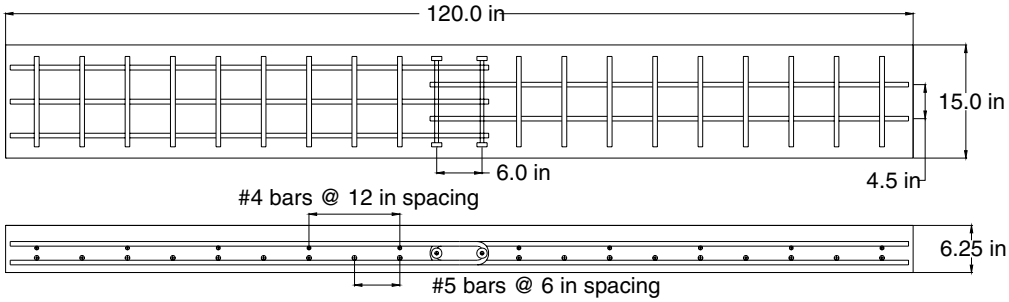

Figure 20 U-bar longitudinal joint specimen.

specimens). The three joint details investigated included (1) lapped headed reinforcement, (2) lapped U-bar reinforcement fabricated with deformed wire, and (3) lapped U-bar reinforcement fabricated with SS. The three specimens tested in flexure were subjected to forces that would be experienced in a longitudinal deck joint, and three specimens tested in tension were subjected to forces that would be experienced in a transverse joint over an interior pier.

Based on the performance of the initial tests conducted on the U-bar detail (with DWR and SS) for the longitudinal joint shown in Figure 20, and headed reinforcement details for the longitudinal joint shown in Figure 21, the most promising connection concept in terms of behavior, constructability, and cost (the U-bar detail), was investigated in additional tests where parameters were varied to refine the proposed connection concepts.

The capacities of the joint details were used for comparison and the selection of the best performing joint detail. All joint details produced adequate capacities and ductility in both the tension and flexural tests. Specimens with U-bar details and headed bar details both produced a capacity corresponding to their respective nominal design yield strengths. Because the U-bars had a higher nominal design yield strength (i.e., 75 ksi) than the headed bars (i.e., Grade 60), specimens containing the U-bar joint detail produced the largest capacities in both the bending and tension tests without compromising ductility. Smaller crack widths at service-level loading were also produced by the U-bar detail when compared to the headed bar detail.

The constructability and reinforcement costs of the joint details were also compared. The U-bar detail created a less congested joint, which made it the easiest to construct. The bearing heads of the headed bar detail require more space due to the larger diameter of the rebar heads. This extra space reduces construction tolerances and could therefore cause problems in placement of precast deck components. The U-bars can also be easily tied together to form a rebar cage, which would allow for easy construction in the precast yard when compared to the two single layers of reinforcement in the headed bar detail. The lowest material cost was the conventional rebar used for the headed bars. The material costs were competitive between the conventional rebar used in the headed bars and the DWR. The SS reinforcement had the highest cost.

After consideration of capacity, service-level crack widths, constructability, and cost, the U-bar detail, with an overlap length of 6 in., a rebar spacing of 4.5 in., and two transverse lacer bars constructed of DWR was recommended for the second phase of tests.

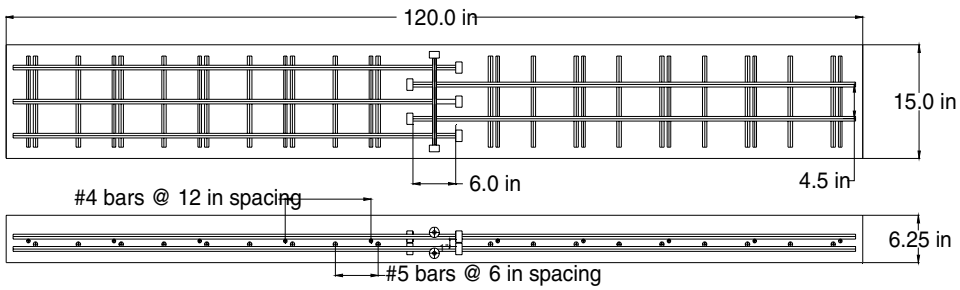

Figure 21 Headed bar longitudinal joint specimen.

Copyright National Academy of Sciences. All rights reserved.

In the second phase of tests, another six specimens with the U-bar detail were tested, three in flexure and three in tension, to investigate effects of variables including overlap lengths, rebar spacings, and concrete strengths. Based on results of the second phase of tests, the following conclusions were made:

By reducing the concrete strength, both the flexural and tensile capacities were reduced. When decreasing the joint overlap length from 6 in. to 4 in., the crack widths were significantly enlarged, the flexural capacity was decreased by 17.8%, and the tensile capacity was decreased by 18.9%. Increasing the spacing of the U-bar reinforcement from 4.5 in. to 6.0 in. was not observed to significantly change the behaviors of longitudinal and transverse joints in terms of their crack widths, flexural capacities, and tensile capacities. In order to provide adequate ductility without significant loss of strength ultimately, the joint overlap length should not be less than 6 in. and #4 lacer bars should be provided to enhance the mechanical anchorage of the U-bars as illustrated in Figure 22.

The lacer bars provided confinement of concrete within the joint and served as a mechanical anchorage for the U-bars. Figure 22 provides an example of the deformation the lacer bars underwent during the tests. The location of the lacer bars in relation to the U-bars enabled the lacer bar to provide bearing to U-bars. These "bearing" forces caused the lacer bar to bend. This interaction between the lacer bar and U-bars helps to explain the greater ductile failure mode observed in the U-bar tests.

Figure 22 Deformation of lacer bar.

In summary, based on capacity, service level crack widths, constructability, and cost, the U-bar detail, with No. 5 equivalent DWR at 4.5-in. spacing with 6-in. overlap length and two transverse lacer bars was recommended for the final longitudinal and transverse joint tests. It should be noted that all of the tests were based on uncoated reinforcement. If epoxy-coated reinforcement were used, larger joint widths may be required to develop the reinforcement across the joint. An alternative to epoxy-coated reinforcement would be to use SS reinforcement, which performed well in the initial study but was an expensive alternative.

In all of the initial tests to select the most viable joint details, the details were cast in monolithic concrete specimens. Prior to testing the details within jointed test specimens, an extensive study was conducted to select high performance durable 7-day and overnight CP materials based on the specified performance criteria developed for freeze-thaw, shrinkage, bond strength, and permeability.

Development of Performance Criteria for CP Materials

For precast bridge deck systems with CIP connections, precast elements are brought to the construction site ready to be set in place and quickly joined together. Then, a concrete CP completes the connection. The performance of the CP material is one of the key parameters affecting the overall performance of the bridge system.

Longitudinal connections between the flanges of DBTs and between precast panels between girders require that the joints must be able to transfer shear and moment induced by vehicular loads. Shrinkage of CP materials and transverse shortening of precast members further subject the joints to direct tension. Freeze-thaw resistance and low permeability of joints are also important. An ideal CIP connection detail emulates monolithic behavior and results in a more durable and longer lasting structure.

Traditionally, different types of grouts have been used as CP materials for precast bridge deck systems with CIP connections. Mrinmay (1986) documented a wide variety of materials used after 1973 to avoid joint failure in CPs. These materials included sand-epoxy mortars, latex-modified concrete, cement-based grout, nonshrink cement grout, epoxy-mortar grout, calcium-aluminate cement mortar and concrete, methylmethacrylate-polymer concrete and mortar, and

Copyright National Academy of Sciences. All rights reserved.

polymer mortar. Epoxy- or polymer-modified grouts can have significant advantages, such as a high strength of 10 ksi in 6 hours, better bond, reduced chloride permeability, and lower shrinkage (Issa et al. 2003) than different magnesium ammonium phosphate (MAP) grouts. However, they are often significantly more expensive and less compatible with surrounding concrete. In addition, if the resin is used in too large of a volume, the heat of reaction may cause it to boil, and thereby develop less strength and lose bond. Cementitious grouts have been used more in precast construction than have epoxy or polymer-modified grouts (Matsumoto et al. 2001). A primary disadvantage of cementitious grouts is the shrinkage and cracking that result from the use of hydraulic cement. Nonshrink grout compensates for the shrinkage by incorporating expansive agents into the mix. With nonshrink grout, the effects of shrinkage cracks or entrapped air on the transfer of forces and bond are minimized, though not eliminated. ASTM C1107 establishes strength, consistency, and expansion criteria for prepackaged, hydraulic-cement, nonshrink grout.

Nottingham (1996) reported that the very nature of portland cement grouts virtually assures some shrinkage cracks in grout joints, regardless of quality control. Prepackaged MAP-based grout, often extended with pea gravel, can meet requirements like high quality, low shrinkage, impermeability, high bond, high early strength, user friendly, and low-temperature curing ability (Nottingham 1996; Issa et al. 2003). Gulyas et al. (1995) undertook a laboratory study to compare composite grouted keyway specimens using two different grouting materials: nonshrink grouts and MAP mortars, in which MAP materials performed better than nonshrink grouts. Gulyas and Champa (1997) further examined inadequacies in the selection of a traditional nonshrink grout for use in shear keyways. The MAP grout outperformed the nonshrink grout in all areas tested, including direct vertical shear, direct tension, longitudinal shear, bond, shrinkage, and so on. Menkulasi and Roberts-Wollmann (2005) presented a study of the horizontal shear resistance of the connection between full-depth precast concrete bridge deck panels and prestressed concrete girders. Two types of grout were evaluated: a latex modified grout and a MAP grout. For both types of grout, an angular pea gravel filler was added. The MAP grout developed slightly higher peak shear stresses than the latex modified grout.

Grout without coarse aggregate extension is usually referred to as neat grout, while grout with coarse aggregate extension, typically ½- or ⅜-in. coarse aggregate, is extended grout. Compared with neat grout, extended grout has the following potential benefits: (1) more compatible with concrete; (2) better interlock between connection components; (3) denser, less permeable; (4) less drying shrinkage and creep; and (5) larger grout volume per bag, hence less expensive. However, it was pointed out by Matsumoto et al. (2001) that the extended grout required more cement paste than available in prepackaged bags, leading to lower strengths and poor workability.

As discussed above, numerous products are available for CP materials, and various materials were studied. However, limited research had been previously conducted to provide consistent comparison among a large number of different types of CP materials. Also, adequate performance-based criteria need to be developed to ensure appropriate selection of CP materials, particularly for accelerated bridge construction. Performance-based specifications focus on properties such as consistency, strength, durability, and aesthetics. They reward quality, innovation, and technical knowledge in addition to promoting better use of materials, and present an immense opportunity to optimize materials design.

As part of the process of developing the performance criteria, eight candidate CP materials were selected and evaluated with respect to their potential effectiveness in accelerated bridge construction. In this context, accelerated bridge construction is defined with respect to two categories: overnight cure of CP materials and 7-day cure of CP materials. For the overnight cure, published performance data from different grout materials were collected through contacts with material suppliers and users. For the 7-day cure, standard or special concrete mixtures and their performance data were collected through contacts with HPC (High Performance Concrete) showcase states as well as with material suppliers. Based on these initial collected data, four grouts were first selected as candidate overnight cure materials, and four special concrete mixes as candidate 7-day cure materials. The preliminary selection was based on strength tests of selected materials or on prediction models to narrow the candidate materials down to two materials in each of the two categories. Then long-term tests were performed on the final four selected materials, including freezing-and-thawing durability, shrinkage, bond, and permeability tests.

For precast bridge deck systems with CIP connections, precast elements are brought to the construction

Copyright National Academy of Sciences. All rights reserved.

Table 3 Proposed performance criteria of CP materials.

Performance Characteristic	Test Method	Performance Criteria		
Compressive Strength (CS), ksi	ASTM C39 modified	6.0 ≤ CS @ 8 hours (overnight cure) @ 7 days (7-day cure)		
Shrinkage[1] (S), (Crack age, days)	AASHTO PP34 modified	20 < S		
Bond Strength (BS), psi	ASTM C882 modified	300 < BS		
Chloride Penetration[2] (ChP), (Depth for percent chloride of 0.2% by mass of cement after 90-day ponding, in.)	ASTM C1543 modified	ChP < 1.5		
Freezing-and-Thawing Durability (F/T), (relative modulus after 300 cycles)	ASTM C666 Procedure A modified	Grade[3] 1	Grade 2	Grade 3
		70% ≤ F/T	80% ≤ F/T	90% ≤ F/T

[1]No S criterion need be specified if the CP material is not exposed to moisture, chloride salts or soluble sulfate environments.
[2]No ChP criterion need be specified if the CP material is not exposed to chloride salts or soluble sulfate environments.
[3]Grades are defined in Table 4.

site ready to be set in place and quickly joined together. Then, a concrete CP completes the connection. The performance of the CP material is one of the key parameters affecting the overall performance of the bridge system. The final performance criteria for selecting durable CP materials given in Tables 3 and 4 were developed based on extensive literature review which included proposals by Russell and Ozyildirim (2006) and Tepke and Tikalsky (2007) and the results of the long-term tests.

Numerical Investigation to Determine Loadings to be Applied in Joint Tests

To determine the service static and fatigue loadings that might be expected in the longitudinal and transverse joint connection concepts, numerical studies of bridge systems were conducted with a number of variations. The analytical parametric study considered parameters such as different loading locations, effect of bridge width, design truck and lane loading versus design tandem and lane loading, girder geometry (depth, spacing and span), bridge skew, single-lane loading versus multi-lane loading, and impact of cracking of the joints. Through this investigation, a database of maximum forces to be expected in the joint was developed. These forces were subsequently used to determine the fatigue loading demand for the large-scale longitudinal joint specimen (flexure and shear-flexure) tests and the large-scale transverse joint specimen (tension) tests.

Large-scale Tests on Longitudinal and Transverse Joints with U-Bar Details and Both 7-Day and Overnight Cure CP Materials

Large-scale longitudinal and transverse jointed specimens were fabricated to investigate the flexure

Table 4 Application of CP material grades for freezing-and-thawing durability.

Freezing-and-thawing Durability (F/T)	Is the concrete exposed to freezing-and-thawing environments?	Yes	Is the member exposed to deicing salts?	Yes	Will the member be saturated during freezing?	Yes. Specify F/T-Grade 3 No. Specify F/T-Grade 2
				No. Specify F/T-Grade 1		
		No. F/T grade should not be specified.				

Copyright National Academy of Sciences. All rights reserved.

and flexure-shear behavior of the longitudinal joints and the tension behavior of the transverse jointed specimens. The tension tests on the transverse jointed specimens were intended to simulate continuity provided by the joints over the piers, where it was assumed that the deck would transmit tension equilibrated by compression in the girder. The large-scale specimens were fabricated with the most promising connection detail, which was a U-bar connection concept fabricated with DWR. The specimens were subjected to static and fatigue tests with the loads determined in the numerical parametric study. The tests were evaluated in terms of load-deformation response, strain distribution, crack control, and strength.

Longitudinal Joint Tests. Figures 23 and 24 show the dimensions and the reinforcement layout in the longitudinal joint specimen. The specimens were fabricated with the U-bars extending out of both faces of the test specimens, such that the specimens could be reused by severing the panel after testing and rotating the panels to fabricate a new joint. Figure 25 shows a profile view of the joint surface before and after sand blasting.

The longitudinal joint was filled with CP material to complete the connection, which simulated the longitudinal joint connection at the interface of the top flange of adjacent DBT girders or full-depth precast

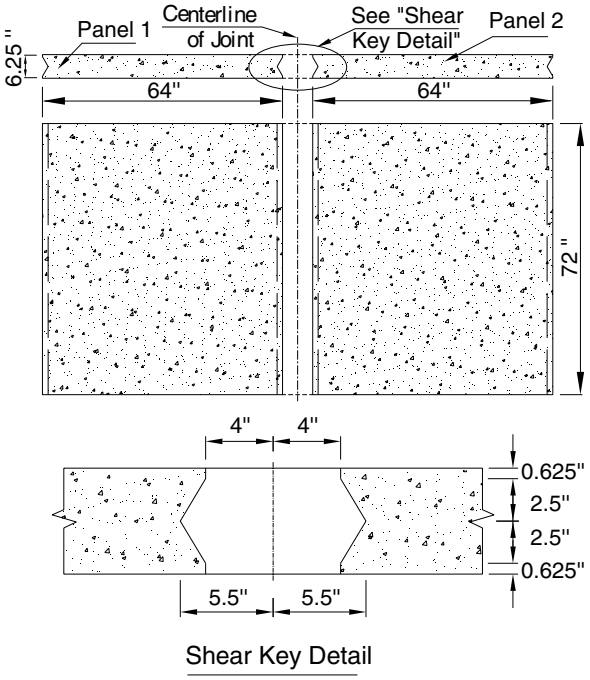

Figure 23 Dimensions of longitudinal joint specimen.

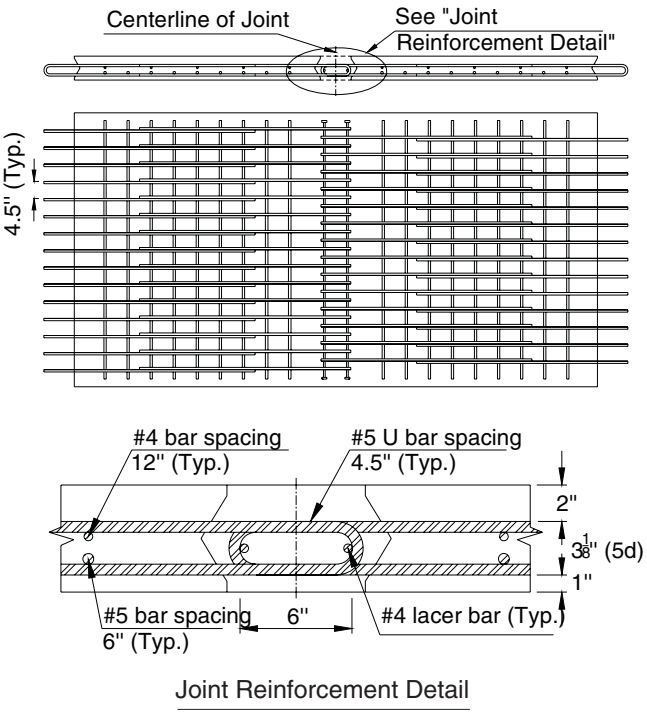

Figure 24 Reinforcement layout in longitudinal joint specimen.

panel-to-panel connections, considered to be the structural element of the bridge deck. To facilitate accelerated bridge construction, it is important for the selected CP material to reach its design compressive strength in a relatively short period of time. In this study, it was decided to use two primary CP materials, SET® 45 Hot Weather (HW) for overnight cure and an HPC mix for the 7-day cure. The grout SET 45 HW used in the longitudinal joint study was investigated both without extension in two joints and with 60% extension in two joints for comparison. The uniform-sized sound 0.25 in. to 0.5 in. round pea gravel used to extend the grouts was tested with 10% hydrochloric acid (HCl) to confirm that it was not calcareous. Figure 26 shows the test specimen before and after grouting. The loading matrix describing the tests conducted on the longitudinal joint specimens is given in Table 5. The test setups used to investigate static flexure (SF), static shear (SS), fatigue flexure (FF), and fatigue shear (FS) are given in Figure 27, parts (a) through (d).

The measured ultimate capacities of all of the specimens obtained following the service fatigue loading cycles exceeded their calculated capacities. The joints with the overnight cure materials had lower capacities than those with the 7-day cure, due to the lower strength of the joint material. Based on the

Copyright National Academy of Sciences. All rights reserved.

(a) Before sandblasting

(b) After sandblasting

Figure 25 Profile of joint surface.

(a) Before grouting

(b) After grouting

Figure 26 Longitudinal joint specimen before and after grouting.

Table 5 Slab specimen loading matrix.

Overnight Cure				7-Day Cure			
Flexure		Flexure-Shear		Flexure		Flexure-Shear	
Static (SF-O)	Fatigue (FF-O)	Static (SS-O)	Fatigue (FS-O)	Static (SF-7)	Fatigue (FF-7)	Static (SS-7)	Fatigue (FS-7)
SET 45 HW extended	SET 45 HW	SET 45 HW	SET 45 HW extended	HPC Mix 1			

NOTE: SF = static flexure, FF = fatigue flexure, SS = static shear, FS = fatigue shear, O = overnight cure, and 7 = 7-day cure.

Copyright National Academy of Sciences. All rights reserved.

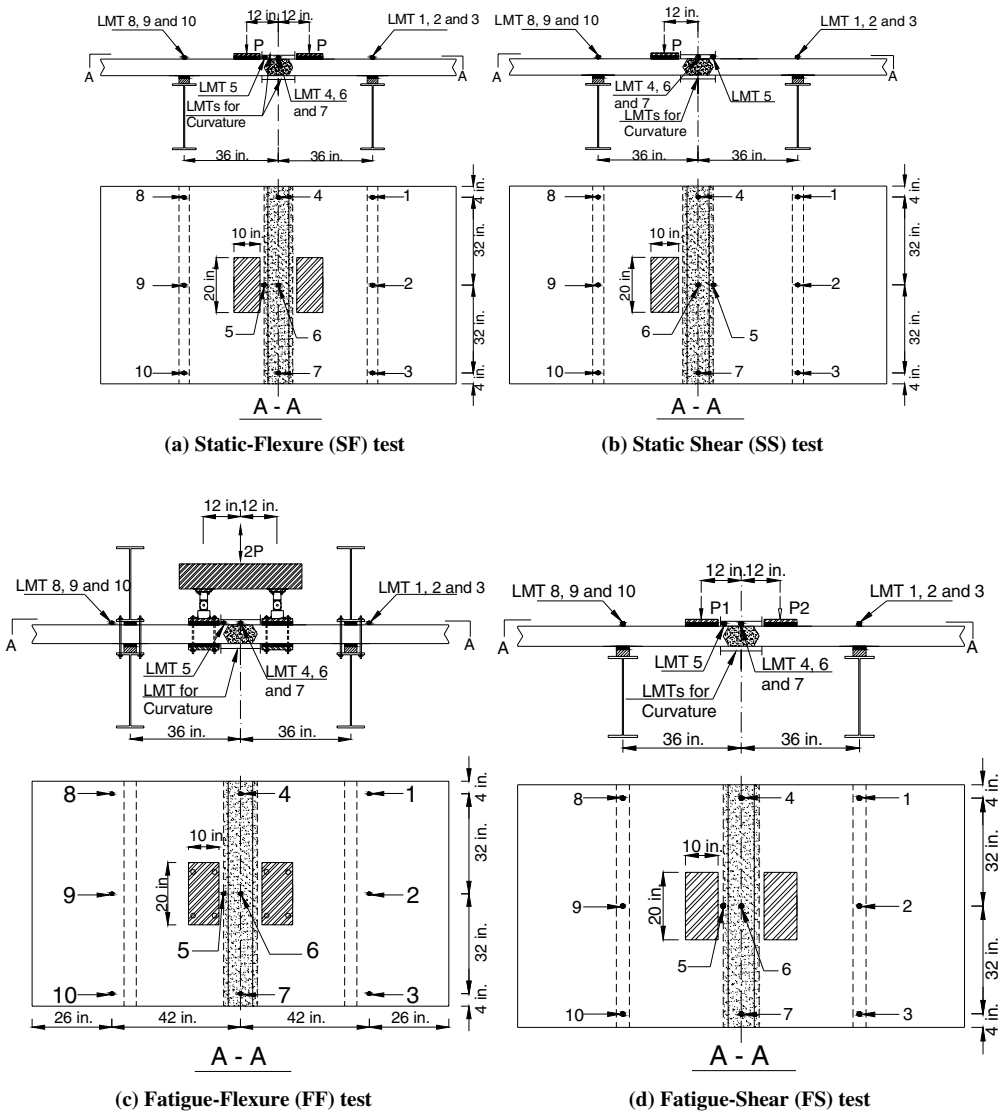

Figure 27 Longitudinal joint specimen test setup.

parametric study and the experimental program, the following findings were made:

- Fatigue loading had little influence on the behavior of the longitudinal joints (flexure and flexure-shear test specimens) in terms of average curvature of the joint, deflection at midspan, relative displacement of the joint interface and joint center, as well as reinforcement strain under service live load.
- Fatigue loading was observed to have an effect on the loading capacity of the flexure specimens using the overnight cure material. After two million cycles, the specimens fabricated with the overnight cure material had less load capacity than the corresponding specimens subjected to the static load tests. For the specimens with 7-day cure material in the joint, fatigue loading had a negligible effect on the results for the flexure-shear tests. In the case of the flexure tests, the failure load was not reached due to limitations of the MTS test equipment.
- Joints with the 7-day cure material performed better than those with the overnight cure material in some cases. Examples included the flexure-shear tests, SS and FS, where the joints with the 7-day cure material had larger failure loads and curvatures than those of the specimen with the overnight cure material. This was because the 7-day cure material used developed higher strengths than could be achieved with the overnight cure material in the tests.

Copyright National Academy of Sciences. All rights reserved.

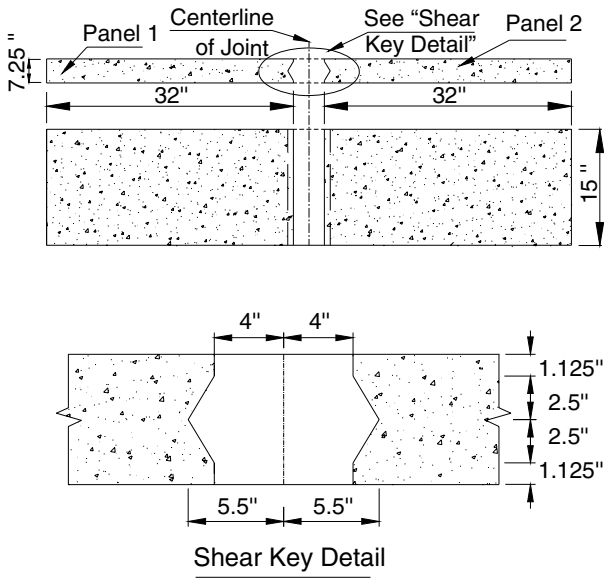

Figure 28 Dimension of transverse joint (tension) specimen.

Based on these tests, the U-bar detail was deemed to be a viable connection system for longitudinal joints between full-depth precast deck panels and DBTs.

Transverse Joint Tests. Figures 28 and 29 show the dimensions and the reinforcement layout in the longitudinal joint specimen. Figure 30 shows a profile view of the joint surface before and after sand blasting. The loading matrix describing the tests conducted on the transverse joint specimens is given in Table 6.

There were four layers of reinforcement in each panel along the specimen depth direction with a 2-in. cover at the top and 1-in. cover at the bottom. The straight bars simulated the transverse reinforcement while the U-bars simulated the longitudinal reinforcement that comprised the transverse joint connection reinforcement in the bridge deck. The reinforcement details in the specimen were as follows: #5 straight bar spaced at 6 in. at the bottom along the specimen width direction and #4 straight bar spaced at 12 in. at the top along the specimen width direction. The #5 U-bars projected out of the panel to splice with the U-bars in the adjacent panel in the transverse joint. The spacing of the U-bars was 4.5 in. and the overlap length (the distance between bearing surfaces of adjacent U-bars) was 6 in. The interior diameter of bend of the U-bar was $3d_b$.

All of the specimens exceeded the nominal service live load capacity. However, only ST-7 and FT-7 exceeded the calculated tensile capacity. It was concluded that tensile capacities were reduced by reducing the concrete strength. Please note that the longitudinal reinforcement was not continuous in the U-bar detail. And one reason that ST-O and FT-O had lower capacities was due to the lower strength of the joint material. Attention needs be paid to the moisture loss during the first 3 hours after placement, which may have caused the lower strengths in the tests.

A similar phenomenon was observed in the monolithic transverse joint specimens. Typically, the tensile capacity of a specimen under pure tension is a function of the amount and strength of steel if

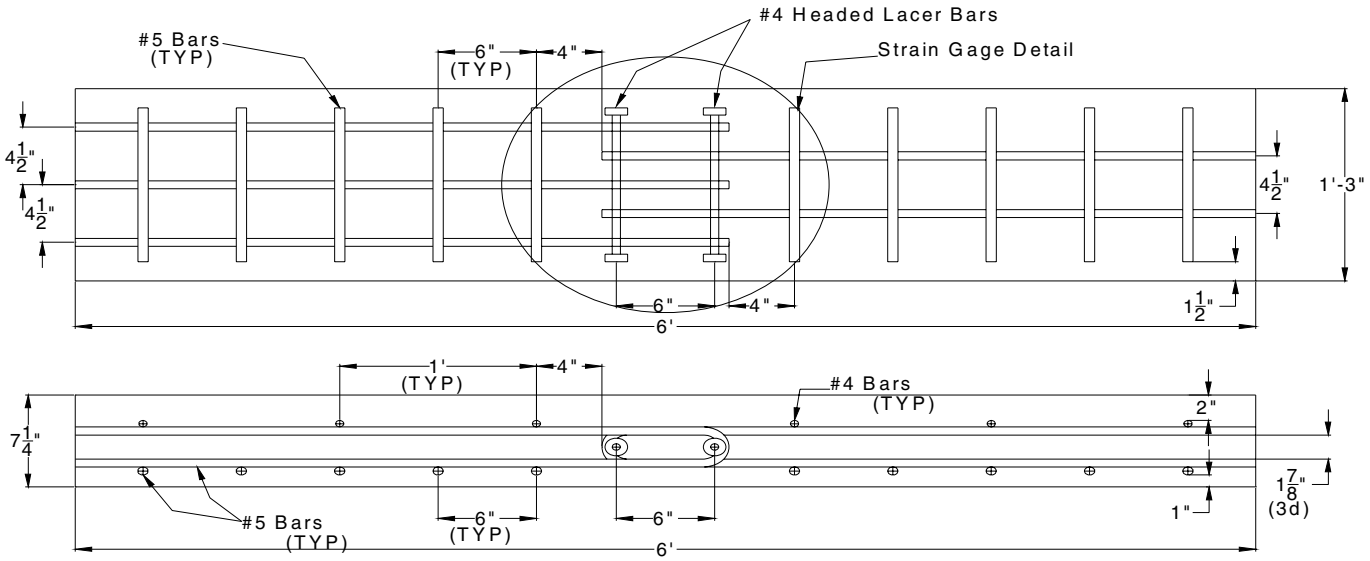

Figure 29 Reinforcement layout in transverse joint (tension) specimen.

Copyright National Academy of Sciences. All rights reserved.

(a) Before grouting (b) After grouting

Figure 30 Transverse joint (tension) specimen before and after grouting.

the steel is continuous. In the earlier tests, all four specimens exceeded the service-level load. However, only two of the specimens exceeded the theoretical tensile capacity. Because the amount of steel was not varied among the test specimens, the tensile capacity was attributed to the interaction between the concrete and steel as well as the steel arrangement. The tensile capacity of the specimen, which had a decrease in f'_c from 10 to 7 ksi, was 4.6% less than the expected capacity based on nominal properties, and the tensile capacity of the specimen that had a decrease in joint overlap length from 6 in. to 4 in. was 18.7% less than the expected capacity based on nominal properties. In the joint zone, the staggered U-bars tied with two lacer bars created a truss-like model. This truss model can also be considered a strut-and-tie model where the compression in the concrete represents the strut and the tension in the reinforcement represents the tie.

The transverse of forces through the joint region to the staggered lapped U-bars needs to be considered in evaluating the tensile capacity.

Table 6 Transverse joint (tension) specimen loading matrix.

Overnight Cure		7-Day Cure	
Static ST-O	Fatigue FT-O	Static ST-7	Fatigue FT-7
SET 45 HW	SET 45 HW	HPC Mix 1	HPC Mix 1

NOTE: ST = static tension, FT = fatigue tension, O = overnight cure, and 7 = 7-day cure.

Based on the parametric study and the experimental program, the following findings were made for the transverse joint specimens:

- The fatigue loading had no significant influence on the tensile capacity and reinforcement strains.
- The fatigue loading was observed to have an effect on the deflection development, particularly for the joints with the 7-day cure material.
- The fatigue loading had some effect on the measured crack widths in the specimens with the overnight cure material. Under the same loading, the crack widths were observed to increase after the fatigue cycles.
- Undesirable wider crack widths will be developed at service-load levels in transverse joints designed with higher grades of steel (e.g., 75 ksi compared to 60 ksi) because smaller amounts of reinforcement can provide the required nominal strength. Under service loads, larger stresses would be expected in the smaller bars, which lead to wider cracks at service. It is recommended that 60 ksi nominal yield strength be used in the design of transverse joints, or that stresses in the reinforcement are limited at service.

Based on these tests and with the aforementioned caveats, the U-bar detail may be considered a viable connection system for transverse joints in continuous DBT and full-depth precast deck panel on girder bridges.

Copyright National Academy of Sciences. All rights reserved.

In summary, the studies indicated that the proposed longitudinal joint detail had sufficient strength, fatigue characteristics, and crack control for the maximum service loads determined from the analytical studies and was deemed to be a viable connection system to provide continuity in jointed deck systems over piers. The tests also confirmed that the U-bar detail was a viable connection system for the transverse joint. The joint with the 7-day cure material was able to achieve higher strengths, which might be attributed to the section with the lower strength overnight cure material being unable to fully develop the reinforcement. To reduce the crack sizes in the joints, it is proposed to reduce the service stresses in the joints. This could be accommodated economically by using more lower-grade reinforcement (i.e., Grade 60 rather than Grade 75 bars).

Conclusions and Recommendations

The research completed under NCHRP Project 10-71 study resulted in the development of a comprehensive design guide for the design and construction of longitudinal and transverse joints for full-depth deck panels and DBTs. The design guide covers the detailing requirements for both loop-bar and headed-bar details. Adequate performance of these systems requires the use of lacer bars which improve the mechanical anchorage of these systems. Tests were conducted to investigate the behavior of these systems in shallow decks to emulate the flanges of DBTs. These shallow deck thicknesses required the use of tighter bends than presently allowed by the bridge design specifications and, thus, the recommendations are restricted to wire reinforcement and SS reinforcement, which may accommodate tighter bends due to their higher levels of ductility. Another important feature of these joints is the performance of the CP materials, which was also investigated through a series of laboratory tests that included an evaluation of the shrinkage and F/T characteristics of candidate overnight-cure and 7-day cure materials that might be considered in rapid construction applications. Three MathCAD examples were developed to illustrate the proposed detailing for longitudinal joints between DBTs, longitudinal joints in full-depth precast panels on girders, and transverse joints.

REFERENCES FOR PCSSS PORTION OF STUDY

AASHTO, 2010, *AASHTO LRFD Bridge Design Specifications,* 5th Edition, Washington, D.C.

ACI 318, 2008, *Building Code Requirements for Structural Concrete and Commentary,* American Concrete Institute, Farmington Hills, MI.

Bell, C., Shield, C.K., French, C.W. (2006), *Application of Precast Decks and other Elements to Bridge Structures.* Mn/DOT Technical Report No. MN/RC 2006-37, Minnesota Department of Transportation, St. Paul.

Eriksson, W.D. (2008), *Vertical Tensile Stresses in End Regions of Precast Composite Slab-Span Systems and Restraint Moments,* MS Thesis, University of Minnesota-Twin Cities Graduate School, Minneapolis.

French, C. et al. (2011), *NCHRP Web-Only Document 173: Cast-in-Place Concrete Connections for Precast Deck Systems.* NCHRP 10-71 Final Report. Transportation Research Board of the National Academies, Washington, D.C., 782 pp.

Frosch, R.J., Bice, J.K., Erickson, J.B. (2006), *Field Investigation of a Concrete Deck Designed by the AASHTO Empirical Method: The Control of Deck Cracking,* Indiana Department of Transportation Technical Report FHWA/IN/JTRP-2006/32. September. Indiana Department of Transportation, Indianapolis.

Molnau, K., Dimaculangan, M.C. (2007), "Inverted T Design." LRFD Bridge Design Workshop, Minnesota Department of Transportation, St. Paul, June 12.

Naito, C., and Deschenes, D. (2006), *Horizontal Shear Capacity of Composite Concrete Beams without Ties, Proc., Precast/Prestressed Concrete Institute (PCI) National Bridge Conference.* Grapevine, TX.

Oesterle, et al. (2009), "Design and Construction Guidelines for Long-Span Decked Precast, Prestressed Concrete Girder Bridges," Final Report, NCHRP Project 12-69. Construction Technology Laboratories, Inc., Skokie, IL.

Smith, M.J. et al. (2008), *Monitoring and Analysis of Mn/DOT Precast Composite Slab Span System (PCSSS),* Mn/DOT Technical Report No. MN/RC 2008-41. September, Minnesota Department of Transportation, St. Paul.

Uijl, J.A.d. (1983), *Tensile Stresses in the Transmission Zones of Hollow-Core Slabs Prestressed with Pretensioned Strands,* Report 5-83-10, The Netherlands: Delft University of Technology Department of Civil Engineering.

REFERENCES FOR LONGITUDINAL AND TRANSVERSE JOINTS IN DBT AND FULL-DEPTH PRECAST PANEL ON GIRDER SYSTEM PORTION OF STUDY

Gulyas, R.J. and Champa, J.T. (1997), "Use of Composite Testing for Evaluation of Keyway Grout for Precast Prestressed Bridge Beams," *American Concrete Institute (ACI) Materials Journal,* Technical Paper, V. 94, No. 3, May–June, pp. 244–250.

Copyright National Academy of Sciences. All rights reserved.

Gulyas, R.J., Wirthlin, G.J., and Champa, J.T. (1995), "Evaluation of Keyway Grout Test Methods for Precast Concrete Bridges," *Precast/Prestressed Concrete Institute (PCI) Journal,* V. 40, No. 1, January–February, pp. 44–57.

Issa, M.A., Cyro do V., Abdalla, H., and Islam, M.S. (2003), "Performance of Transverse Joint Grout Materials in Full-Depth Precast Concrete Bridge Deck Systems," *Precast/Prestressed Concrete Institute (PCI) Journal,* V. 48, No. 4, July–August, pp. 92–103.

Li, L., Ma, Z., Griffey, M.E., and Oesterle, R.G. (2010), "Improved Longitudinal Joint Details in Decked Bulb Tees for Accelerated Bridge Construction: Concept Development," *ASCE Journal of Bridge Engineering,* 15(3), 327–336.

Li, L., Ma, Z., and Oesterle, R.G. (2010a), "Improved Longitudinal Joint Details in Decked Bulb Tees for Accelerated Bridge Construction: Fatigue Evaluation," *ASCE Journal of Bridge Engineering,* 15(5), 511–522.

Ma, Z. et al. (2007), "Field Test and 3D FE Modeling of Decked Bulb-Tee Bridges," *ASCE Journal of Bridge Engineering,* 12(3), 306–314.

Martin, L.D., and Osborn, A.E.N. (1983), *Connections for Modular Precast Concrete Bridge Decks,* Report No. FHWA/RD-82/106, United States Department of Transportation, Federal Highway Administration.

Matsumoto, E. et al. (2001), "Development of a Precast Bent Cap System," Project summary report 1748-S, University of Texas Austin, March.

Menkulasi, F. and Roberts-Wollmann, C.L. (2005), "Behavior of Horizontal Shear Connections for Full-Depth Precast Concrete Bridge Decks on Prestressed I-Girders," *Precast/Prestressed Concrete Institute (PCI) Journal,* V. 50, No. 3, May–June, pp. 60–73.

Mrinmay B. (1986), "Precast Bridge Deck Design System," *Prestressed/Precast Concrete Institute (PCI) Journal,* V. 31, No. 2, March–April, pp. 40–86.

Nottingham, D. (1996), "Joints Grouting in Alaskan Bridges and Dock Decks," *Concrete International,* V. 18, No. 2, February, pp. 45–48.

Russell, H.G. and Ozyildirim, H.C. (2006), "Revising high performance concrete classifications," *Concrete International,* August, pp. 43–49.

Stanton, J.F., and Mattock, A.H. (1986), *NCHRP Report 287: Load Distribution and Connection Design for Precast Stemmed Multibeam Bridge Superstructures,* TRB, National Research Council, Washington, D.C.

Tepke, D.G. and Tikalsky, P.J. (2007), "Best Engineering Practices Guide for Bridge Deck Durability Report," Report no. PTI 2007-63. Pennsylvania Transportation Institute, University Park, 31 pp.

Copyright National Academy of Sciences. All rights reserved.

TRB

Transportation Research Board
500 Fifth Street, NW
Washington, DC 20001

THE NATIONAL ACADEMIES™
Advisers to the Nation on Science, Engineering, and Medicine

The nation turns to the National Academies—National Academy of Sciences, National Academy of Engineering, Institute of Medicine, and National Research Council—for independent, objective advice on issues that affect people's lives worldwide.
www.national-academies.org

ISBN 978-0-309-21328-8
90000
9 780309 213288

Subscriber Categories: Highways • Bridges and Other Structures

These digests are issued in order to increase awareness of research results emanating from projects in the Cooperative Research Programs (CRP). Persons wanting to pursue the project subject matter in greater depth should contact the CRP Staff, Transportation Research Board of the National Academies, 500 Fifth Street, NW, Washington, DC 20001.

COPYRIGHT INFORMATION

Authors herein are responsible for the authenticity of their materials and for obtaining written permissions from publishers or persons who own the copyright to any previously published or copyrighted material used herein.

Cooperative Research Programs (CRP) grants permission to reproduce material in this publication for classroom and not-for-profit purposes. Permission is given with the understanding that none of the material will be used to imply TRB, AASHTO, FAA, FHWA, FMCSA, FTA, or Transit Development Corporation endorsement of a particular product, method, or practice. It is expected that those reproducing the material in this document for educational and not-for-profit uses will give appropriate acknowledgment of the source of any reprinted or reproduced material. For other uses of the material, request permission from CRP.

Copyright National Academy of Sciences. All rights reserved.